European Community's Framework Programme 6

EUROPEAN EXTREMELY LARGE TELESCOPE DESIGN STUDY

Document title:	*SCELT – a sub-millimetre camera for the ELT*
Document number:	ELT-TRE-PPP-11170-00001
Issue No	0.14 **DRAFT ONLY**
Date	

Prepared by

Approved by

Released by

CHANGE RECORD

Issue	Date	Section / Paragraph affected	Reason / Initiation / Remarks

Contents

Abbreviations

EC	European Commission
ELT	Extremely Large Telescope
ESO	European Southern Observatory
FP6	Framework Programme 6
N/A	Not applicable
TBC	To Be Confirmed
TBD	To Be Determined
WBS	Work Breakdown Structure
WP	Work package
AIV	Assembly, Integration & Verification
CA	Clear Aperture
DRF	Dilution Refrigerator
FNO	Field Number
FoV	Field of View
FPU	Focal Plane Unit
GM	Gifford-McMahon
KIDs	Kinetic Inductance Detectors
LN2	Liquid Nitrogen
NEFD	Noise Equivalent Flux Density
NEP	Noise Equivalent Power
NIST	National Institute of Standards and Technology
PCB	Printed Circuit Board
PTC	Pulse Tube Cooler
PWV	Precipitable Water Vapour
SCELT	Sub-mm Camera for ELT
SED	Spectral Energy Distribution
SMC	Scottish Microelectronics Centre
SQUID	Superconducting Quantum Interference Device
TES	Transition Edge Sensor
UK ATC	United Kingdom Astronomy Technology Centre

1 Executive summary

This document describes an initial concept for a large-format sub-millimetre camera to be used on the European Extremely Large Telescope. Such an imager – dubbed SCELT – will concentrate on a relatively unexplored region of wavelength space, the atmospheric windows at 350 and 450μm. SCELT will have a 5 arcminute field-of-view and will generate diffraction-limited images simultaneously at 450 and 350μm and, optionally, 850μm. The large primary of ELT provides SCELT with high sensitivity whilst avoiding the background confusion limits of smaller telescopes.

The results from such an instrument will impact a wide range of research areas, and would help answer some of the most fundamental questions about the origin of dust, planets, stars and galaxies. For example, SCELT would be able to detect dust in normal Milky Way Galaxies throughout the Universe, or in "normal" planetary systems similar to our own Solar System within 10pc. We believe that the scientific return from the ELT would be significantly increased by the inclusion of a sub-millimetre imager. Some key questions which SCELT would help answer are:

- Why is our Solar System so free of dust? Do we live in an unusual planetary system?
- What is the origin of the Kuiper Belt?
- How do brown dwarfs form?
- How is the clump mass function in clouds related to the stellar IMF? Does this hold for very high and low masses?
- Where is the bulk of dust in Galaxies? Is there a massive additional "cold, dark" component?
- What is the star formation history of different types of Galaxies?
- How was dust formed in the early Universe?
- What is the origin of the low-level sub-mm background?

SCELT is highly complementary to ALMA, extending its sensitivity out to large-scale structure, as well as providing targets for ALMA followup. For relatively little money compared with the cost of ALMA, astronomers with access to SCELT will have a unique advantage over other ALMA users.

A critical aspect affecting the sensitivity of SCELT is the amount of atmospheric precipitable water vapour, directly related to the site quality. *This is more important than the telescope diameter.* At 450μm for example, SCELT using a 30m telescope on a good site (0.5mm pwv) will be as sensitive as a 42m telescope on a mediocre site (1mm pwv), and more sensitive than a 60m primary on a poor site (2mm pwv). *A clear outcome of this report is that the ELT should be on the driest possible site.*

The subsequent engineering approach to fulfil the SCELT science case has been to provide a basic concept taking advantage of the technology and methodology being developed for SCUBA 2 - now considered the cutting edge of sub-mm instrumentation. Where it is likely that technology emerging in the next few years might offer significant advantages in an instrument being built on the timescale of the ELT, this has been identified. An example of this is large-format detectors. Areas where a dedicated R&D approach would be needed are also identified (e.g. development of filter manufacturing capability).

2 Applicable Documents

The following applicable documents of the exact issue shown form a part of this plan to the extent specified herein. In the event of conflict between the documents referenced herein and the content of the present plan, the content of the present plan shall be taken as superseding requirement.

	Title	Number & Issue
AD01	ELT Instrumentation Sub-millimeter Camera for ELT Technical Specification and Statement of Work	ELT-SPE-ESO-00000-0155 Issue 1.0 dated 22 Dec 2005
AD02	ELT Telescope-Instruments Interface Control Document	ELT-ICD-ESO-00000-0139 Issue 1.1 dated 25 Jan 2005
RD01	SCELT: a large format sub millimetre camera on the Overwhelmingly Large Telescope Holland et al	SPIE 4840, 340
RD02	A large single-aperture telescope for sub millimetre astronomy Holland et al	SPIE 5489, 61
RD03	Adaptor-rotator draft concept	N.B. by S. D'Odorico -6 Jun 2005
RD04	Total power atmospheric phase correction at the SMA. Memo 154	Battat, Dec 2004
RD05	Note on "ELT Adaptive Optics Requirements for TELT/SCELT"	Email, V1.0, May 19, 2005
RD06	SCUBA-2 Array Technology Proof-of-Concept	Nov. 2002
RD07	Theoretical Modelling of Optical and X-ray Photon counting Kinetic Inductance Detectors. George Vardulakis, Stafford Withington, David Goldie	May 2005 SPIE 5499..348 2004
RD08	Frequency domain multiplexing readout of Kinetic Inductance detectors: Naidu Bezawada (UKATC)	May 2005
RD09	Multiplexable Kinetic Inductance Detectors: .B.A. Mazin, P.K. Day, J.Zmuidzinas, and H.G. Leduc	AIP Conf. proc.605, pp.309-312, AIP, New York, 2002

RD10	Superconducting Kinetic Inductance Photon Detectors: B.A. Mazin, Peter K. Day, Henry G. LeDuc, Anastasios Vayonakis and Jonas Zmuidzinas	SPIE 4849..283 2002
RD11	OWL Instrument Concept Study – SCOWL:	OWL-CSR-ESO-00000-0163

3 Science Case

The following sections outline some of the novel and exciting science that could be done with SCELT. The ELT is likely to be built around the middle of the next decade, so these cases are based on projects in areas of current interest, along with some possible projected future science. It is not meant to be a "roadmap" of sub-millimetre science in the next decade, but is structured to give an idea of the burning questions in astronomy that could be uniquely answered by SCELT. However, the orders of magnitude improvements afforded by SCELT is likely to open up new research areas in the submillimetre not even thought of at the present. For each topic, we summarise a list of the specifications and requirements placed on the instrument.

3.1 Baseline system assumptions

For the science cases, we have made some initial assumptions about the telescope design, operation and site quality, as follows.

	Baseline value	Notes
Aperture (D)	42m	Also look at 30m option
Aperture efficiency (η_a)	0.8	Surface is effectively perfect at this wavelength, so η_a is limited by surface losses, geometrical blocking, and segment gaps.
"Workhorse" wavelengths	450μm 350μm	Possibly also 850μm On good sites also 200μm.
Beam size (fwhm)	2.6, 2.1 arcsec	At 450 and 350μm
"Typical" precipitable water vapour content	0.5mm	PWV is lower than this for at least 25-50% of time
Field of view	5 x 5 arcmin	Larger fov would allow faster mapping
Pixel spacing	Nyquist sampling (0.6λ/D)	Assumes pixels can be closely packed
Pixel coverage	100% at all wavelengths	Fraction of science fov that is covered by Nyquist-sampled pixels
Pointing/tracking accuracy	Better than 0.2"	1/10 of the smallest beam size
Strehl ratio	>>80% Strehl ratio over full fov	
Observing time available for SCELT	>30 nights	Number of nights per year when conditions are suitable for operation at "workhorse" wavelengths, and when telescope is not used for other work.

Table 1 Baseline system assumptions

3.2 Reference Science Cases

3.2.1 Solar system

As well as the Planets and Moons, the Solar System contains a significant mass of smaller objects such as Asteroids and Comets. *Understanding these objects is key to understanding the origin of the Solar System.* They can be subdivided into several different populations, such as Centaurs, TNOs, Plutinos, Scattered Disc Objects, KBOs; some are considered primordial from the formation of the Solar System, and others secondary, formed as the result of collisions. We need to explain the differences and origins of these populations, and how the objects are related.

To answer these questions we need to know:

- What are the size distribution and albedo of the populations? What are their total masses? With only optical/ir observations, the size can only be guessed at by assuming a fixed Albedo (e.g. Bernstein et al., 2004).
- What are the surface/regolith properties, such as thermal inertia, roughness and emissivity?
- What is the link to the short period comets?

Answers to these questions will come from study over a wide wavelength regime. Sensitive submm data are critical to understand and model the SEDs.

3.2.1.1 The Outer Solar System: Kuiper Belt Objects

The Kuiper Belt lies at ~30 to possibly >100au from the Sun, resulting in equilibrium temperatures of ~20-40K. *The submm is therefore the key wavelength regime for study of Kuiper Belt Objects.* The critical measurement of the size and Albedo of KBOs is possible by measuring fluxes at both optical and submm or far-IR wavelengths (e.g. Jewitt et al 2001). Currently this can be done on the very rare giant KBOs such as Sedna or Varuna, of diameters ~1000km or larger. But their rarity means we may not be looking at where most of the mass of KBO material lies. Using the SCELT sensitivity coupled with improved optical instruments, we can use this technique to study objects and derive the size distribution down to as small as 100km at distances of 50au. This size regime is very interesting for several reasons: as well as containing most of the KBO mass, it is below the cutoff diameter where bodies are no longer held together by gravitational force (e.g. Pan & Sari, 2005). They are approaching the sizes of classical comets, and may be the link between the two.

It is increasingly apparent that very distant bodies of masses at least that of Pluto do exist at the outer edge of the Kuiper Belt (eg Rabinowicz, et al., astro-ph/0509401). With SCELT there is also an opportunity for serendipitous discovery of distant giant KBOs in the submm; this might be done during large-scale deep cosmological surveys taken over prolonged periods.

3.2.1.2 Asteroids

The submm fluxes of objects in the Asteroid Belt will allow us to measure sizes down to ~20m using a similar technique as described above. Furthermore the submm fluxes and

SED can be used to estimate the surface properties of the regoliths, and the improved sensitivity will enable this to be done over a wide range of size scales.

3.2.1.3 Dust bands

Discovered by IRAS, these are the remains of collisions or breakup of comets and asteroids, and therefore may be local examples of "debris discs". Large-scale mapping of their structure and study of the more distant fainter, cooler bands would be possible. This will help understand the dynamics of these around external planetary systems.

Table 2: requirements from Solar System science

Parameter	Requirement	Desirable	Notes
Wavelength	350μm 450μm	850μm	To get temperature of black-body emission
Sensitivity [1]	<0.1mJy (10σ)	<0.05mJy (10σ)	
Resolution	<2" at workhorse bands	1"	To avoid confusion limit
Field of view	20x20 arcsec		Not critical, as unresolved

3.2.2 Debris discs

At least 15% of main sequence stars are surrounded by dust that has been formed very recently, ie within the last few million years. The source of grains is thought to be mutual collisions and grinding down of larger bodies such as asteroids & comets. Objects such as asteroids in these systems are far too small to be seen directly, making this indirect detection critical for understanding the population of such bodies. Moreover, the distribution of the remnant dust is sculpted by orbital interaction with planets; from the resulting structures we can derive planetary masses and orbits, as well as their migration history (e.g. Wyatt, 2004). So the study of debris discs tells us not only about the dust content of exoplanetary systems, but also about objects all the way from planetary down to asteroids masses.

[1] "Sensitivity" in this and subsequent specification tables refers (except where noted) to the per pixel sensitivity at the "workhorse" wavelength after a "reasonable" amount of observing time, pointing at the same point on the sky (ie neglecting mapping requirements). "Reasonable" means up to a few hours of observing.

Existing studies of debris discs have been severely limited by three effects: instrument sensitivity, confusion against the nearby stellar photosphere, and background confusion. Consequently it has only been possible to investigate those with unusually high dust content, such as Fomalhaut and ε Eri (see

Figure 1). The high sensitivity and spatial resolution of SCELT will revolutionise this; Figure 2 shows that SCELT will be able to detect an ε Eri disc at many hundreds of pc, and discs with dust masses as low as 10^{-5} M_{Earth} at a distance of up to ~8pc around G stars. This lower mass limit is particularly interesting, as it is the mass of dust in our own Solar System's Kuiper Belt – a system apparently relatively free of dust and without a recent major collision. The number of targets within these distances is significant – see Table 3, and thus SCELT will allow for the first time a snapshot of planetary systems in *all* stages after collisions and dust formation, from the extreme cases like Vega and Fomalhaut, down to the dust-poor systems like our own. An intriguing question to answer will be whether *most* stars have some debris, indicative of planets and asteroids? With SCELT we will be able to answer this.

An additional important contribution from such a survey is that missions such as Darwin/TPF will be significantly more sensitive to Terrestrial planets in systems with the lowest dust masses ($<10^{-5}M_{Earth}$; Beichman et al.., 2004). SCELT will be an important pathfinder instrument for target selection.

Table 3: Number of potential targets for detecting Solar System dust masses (based on data from http://nstars.arc.nasa.gov). Assumed 450μm observations.

Spectral type	Luminosity (L_{sol})	Distance limit for detection of 1 Solar System dust mass	Predicted number of targets
F0	9	10	
G2	1	8	20
K0	0.4	5	20
M0	0.1	3	10

SCELT will be able to discriminate against stellar photospheric confusion, as the beamwidth (~2") will spatially resolve typical debris discs out to ~50pc. This ability to avoid confusion from the nearby stellar photosphere is one of the major advantages of SCELT on a large telescope when compared with the >10 arcsec beams of far-IR facilities (ie 4m-class satellites, e.g. Decin, et al., 2003) and existing submm telescopes.

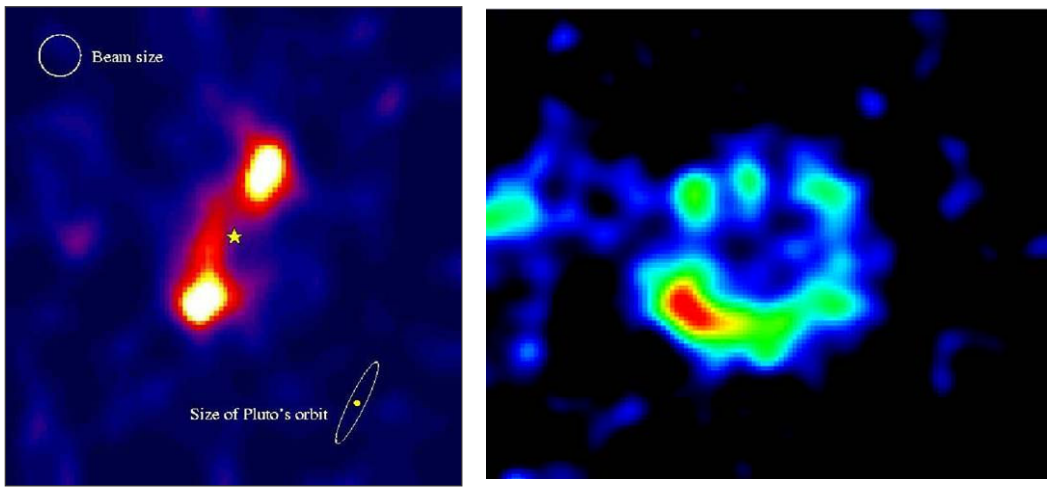

Figure 1: SCUBA images of Fomalhaut and ε Eridanus, two of the closest, brightest and highly-dusty debris discs – at 850um. Resolution is 14 arcsec, or 45au at the distance of ε Eri (3.2pc). SCELT will resolve such discs to distances of 50pc, with and detect masses 100-1000x lower – around that of the Solar System.

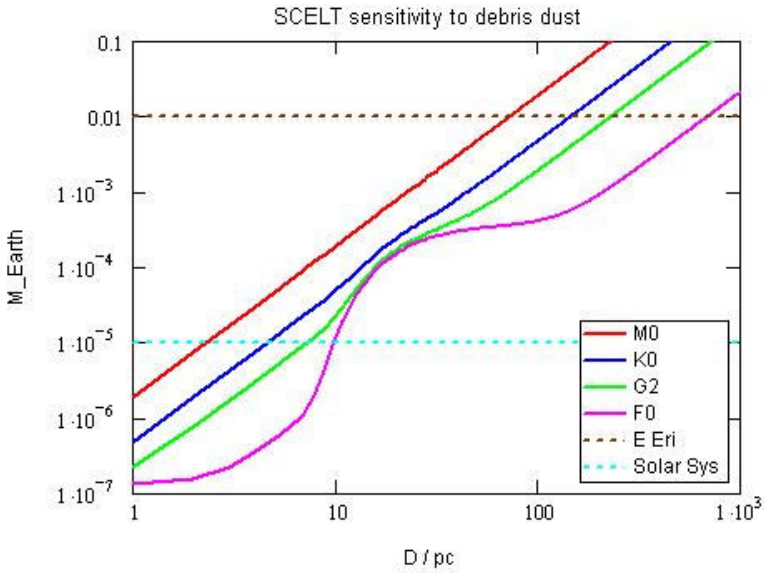

Figure 2: Solid lines represent the detection limit of SCELT (5σ) as a function of distance, for different stars, with 4 hours of integration time. Vertical axis is dust mass in units of Earth masses. The upper and lower dashed lines are the dust masses of E Eri and the Solar System respectively.

It has recently been shown by Spitzer that far and mid-infrared images of debris discs often bear little resemblance to the sub-mm images (Su et al., 2005); this is because the dust emitting at shorter wavelengths is significantly smaller and is blown out by radiation pressure. Even in the sub-mm, the detailed structure at 850μm can be subtly different from that at 350μm (eg Figure 3). With sufficient s:n, the details of these structures can be used to derive important physical information such as the grain sizes, and the physical importance of radiation pressure, PR drag. In the sub-mm grains of size ~1mm (or larger)

dominate; these are relatively unaffected by radiation pressure and so show the complex morphology seen in

Figure 1 and 2. To observe the large (mm to μm) grains trapped in resonances with planets or in rings, we must observe in the mm or sub-mm (e.g. Wyatt et al., 2005, Su et al., 2005). The wavelength of SCELT will therefore provide a unique combination of high sensitivity and sufficient resolution to study these grains in all nearby stars. The changes in morphology indicate that multi-wavelength capability would be important for SCELT.

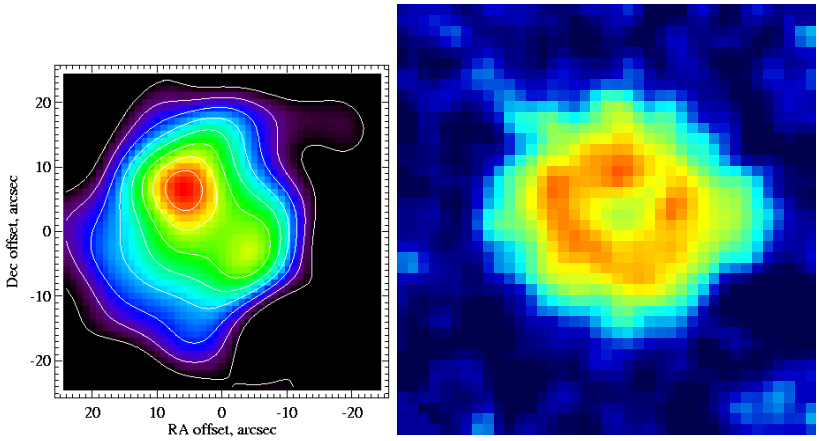

Figure 3: Comparison of Vega images at (left) 850μm and (right) 350μm. From Holland et al. (1998) and Marsh et al. (2006). The morphology of the debris is clearly different at the two wavelengths.

Some of the key questions to answer are:

- Do *all* stars have debris (and by inference, asteroids)?
- Is the Solar System an unusually dust-free case, or is there a continuous distribution of dust masses?
- What is the typical long-term evolution of debris around stars? Spitzer suggests that little changes after the first ~200Myrs of a stars' life, apart from random collisions; however, this is sensitivity-limited. A deep survey is required over a wide age range.
- Does the stellar location and evolution affect the debris disc? Are stars formed in dense environments more likely to have debris?
- Does the stellar mass, metallicity and multiplicity affect debris mass?
- How is the dust alignment affected by the stellar magnetic field (through submm polarimetry – see section 0)

By combining debris disc studies with the direct optical/infrared observations of planets planned with ELT, we will obtain a complete inventory of the rocky and gaseous bodies in these planetary systems.

Table 4: requirements from debris disc science.

Parameter	Requirement	Desirable	Notes
Wavelength	450μm 350μm (simultaneously)	850μm 200μm	Multiple λ to get SEDs
Sensitivity	<0.3mJy (10σ) at 450μm	0.1mJy (10σ) at 850μm <2mJy at 200μm	
Resolution	<3" at workhorse band	2"	For discrimination against photosphere
Field of view	2x2 arcmin	5x5 arcmin	Nearest discs are ~60-100" diameter
PSF accuracy	Can be calibrated (i.e. is stable) to better than 1% over region from 1-10 arcsec	Better than 0.5% over 1-60 arcsec	To allow measurement of faint emission near star, the sidelobes must be low level, and stable.
Observing mode	Mapping FoV	hitchhiker mode preferred	

3.2.3 Planet formation

3.2.3.1 Transitional discs – the last stages of planet formation

The last vestiges of primordial circumstellar discs, around stars of 1Myr to a few 100Myr, are of great interest, as it is in these that planets will be forming. In our own Solar System, this came to an end with the "Age of Heavy Bombardment", where the planets had formed and were impacted by large bodies from the remnant disc. As well as understanding this formation mechanism itself, we also need to explain the evolution from this to the population of evolved exoplanets: how does this dust disappear?

Key questions in this area are:

- What are the timescales of dust removal around young stars? Does the primordial dust exist for prolonged times around stars? How is this dust related to the "age of heavy bombardment" in the Solar System, and is such a phenomenon common to most young planetary systems?
- What is a "typical" planetary system, and how does it get to its current state?
- What is the fundamental origin of the distribution of planetary masses and distance? How is this related to conditions and evolution in the early disc?

- Why do many exoplanets have high eccentricity? Is the Solar System rare in its low planetary eccentricities? This may be related to the prevalence of dust/gas during the early phase of a planet's life.

3.2.3.2 Disc evolution

It is becoming recognised that the evolution of young stars can be widely different: Weak-line T Tauri stars can have little dust compared to their Classical counterparts, yet be of the same age. Why do some stars lose their disc within the first 10^5 yrs, yet others have ones that last for 10Myr or more? Also there is clear evidence that large grains (≥1mm) do exist in many older discs (e.g. Testi et al., 2003): one of the clearest ways to measure this is by looking at the sub-mm spectral slope. However, it is unclear whether this indicates gradual grain growth, or different balances between coagulation and fragmentation (Dullemond & Dominik, 2005). What might affect such balance differently in different objects is unknown, but both effects are likely to have profound impacts on the formation of any larger bodies within these systems.

To answer these questions, deep, whole-cluster surveys are required to track the statistics of all cluster members, with total masses down to the substellar limit. Clusters have sizes of a few arcmin up to ~1 degree for the closest (150pc, Figure 5).

Table 5: requirements from disc science

Parameter	Requirement	Desirable	Notes
Wavelength	350μm, 450μm, 850μm	200μm	Multiple wavelengths to get SED
Sensitivity	<1mJy (10σ) at 450μm <0.2mJy at 850μm	<1mJy at 350μm <3mJy (10σ) at 200μm	
Resolution	2" at workhorse band	1"	Confusion limit in crowded clusters
Field of view	5x5 arcmin	10x10 arcmin	Wide-field mapping of 1-300Myr clusters

3.2.4 Star formation

text needs updating , and with revised sensitivities

3.2.4.1 Formation of the lowest mass stars

What is the mass function of protostellar clumps down to the sub-stellar limit? Does this affect the IMF of stars, potentially explaining the so-called "free-floating" planets? This requires large-scale, deep and high-resolution surveys of the closest star formation regions. Currently the deepest large-scale maps reach 10σ limits of ~0.1Jy at 850μm (e.g. Johnstone et al., 2000). With SCELT, we can reach 10σ limits of 1mJy – *at 450μm* (where

the dust flux is higher) – and covering 1 degree square in a few hours (and a factor of 2-3 lower at 850μm). At this level, the main limitation will be confusion from the background galaxies; techniques such as differential number counts compared with nearby clear sky, and source identification through submm colours (which by that time should be accurately known through templating), will be used to help reduce this confusion limit. The pure sensitivity limit corresponds to a 10σ detection of a $0.1M_{Jupiter}$ clump in Orion. So with SCELT we will be able to extend the clump mass spectrum in Figure 4 down by a factor of ~100, and possibly 1000. *SCELT will provide a complete clump census down to planetary masses in regions out to 2kpc.*

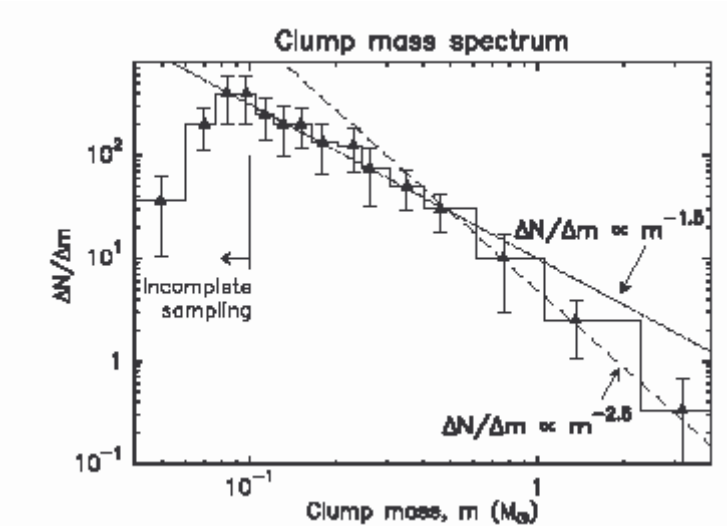

Figure 4 The clump mass spectrum of cores in Ophiuchus (from Andre et al., 1998). Note that this is incomplete below $0.1M_o$.

3.2.4.2 Solar-mass star formation

It is clear that the ability to map star forming regions in the submm dust continuum has provided extremely valuable insights into *local* star formation (i.e. in low-mass formation in clusters within 150pc, and high-mass formation within ~500pc). This is illustrated by the map of ρ Ophiuchus (Figure 5). But we need to extend these local studies to understand star formation in the Galactic context. The combination of sensitivity, reasonable resolution and wide-field mapping with SCELT will allow for the first time, surveys of clusters as far as the Galactic Centre. The deepest studies of Brown Dwarfs in the nearby Trapezium cluster indicate a mean stellar separation of ~0.04pc (Lucas et al., 2005); this would correspond to 1 arcsec at the Galactic Centre. Cluster sizes of a few arcmin could be mapped to 1mJy (10σ), corresponding to $10M_{Jupiter}$ at this distance.

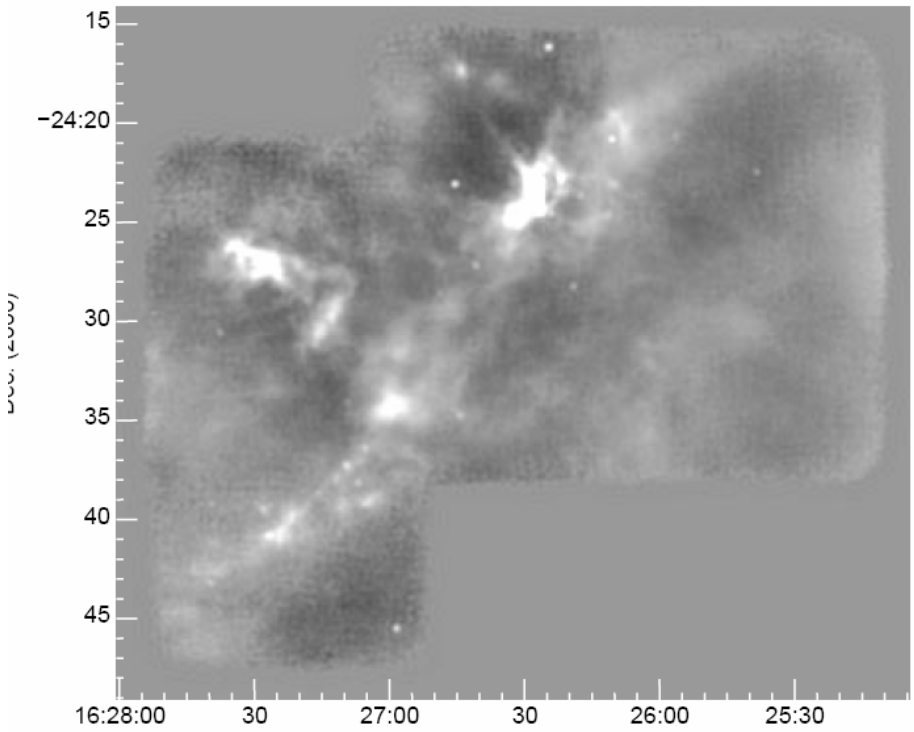

Figure 5: SCUBA map of nearby star forming region (rho Ophiuchus, from Johnstone et al., 2000). 55 cores down to masses of 0.02Msol are identified in this image. SCELT will be able to study clusters similar to this throughout most of the Galaxy.

Some of the key areas to study:

- How do the very lowest mass stars form?
- What determines the minimum mass of a star?
- How do binary stars form? Is it by turbulent fragmentation as suggested by models?
- What is the difference between high and low-mass star formation processes?
- How is the star formation process affected by metallicity and turbulence?

- What are the important parameters affecting star formation in clusters? Is cluster density important in YSO evolution?
- Over what mass range does the mass function of cloud clumps ttrace the initial mass function of stars?
- What are the lifetimes of the different phases of stars formation? Are these affected by parameters such as environment?

3.2.4.3 Proto-binary systems

Most stars form in some kind of binary or higher-multiple system, but the evolution of proto-multiples is very poorly known. At early times, the protostars share a common circumstellar envelope or even a circumbinary accretion disk, but arcsecond resolution is needed to image such systems. Nearby star formation regions such as those in Ophiuchus and Taurus (150pc distance), so wide proto-binaries (~1000 AU) would easily be resolved with an arcsecond ELT beam (corresponding to 150 AU). Furthermore, the sensitivity would be greater than that available with interferometers (e.g. ALMA), with the advantage that large-scale emission would be detected directly. This will give a unique picture of the earliest stages of a proto-multiple star system as it emerges from the parent cloud, and vital clues to how the multiplicity is determined (e.g. by core fragmentation). These studies would quantify the protostar numbers and masses within a group down to very low (sub-stellar) limits, and also show whether the inter-star spacings evolve with time. For example, dynamical interactions may eject group members even at the earliest protostellar stages.

3.2.4.4 Controlling the Interstellar Medium: High-mass star formation

Massive stars are rare, but their effect on the ISM is dramatic. Their winds and outflows are thought to define the lifetime of Giant Molecular Clouds, limiting the possibilities of subsequent star formation, and controlling disc and planet formation around stars in clusters such as Orion. *Any global model of star formation, and any model of Galaxy formation requires an understanding of high-mass star formation.* However, the early stages of high-mass star formation are not understood, partly because they are so fast and consequently rare. A full census of all high-mass star formation throughout the Galaxy will be feasible with SCELT, as the 1" resolution will resolve OB clusters to 20kpc. The resultant statistics will show the rarest of phases, and allow us to understand what defines the highest-mass end of the stellar IMF.

Table 6: specifications from star formation science

Parameter	Requirement	Desirable	Notes
Wavelength	350μm 450μm	850μm 200μm	To get more accurate mass, need 850μm flux as well, to be less dependent on temperature.
Sensitivity	1mJy (10σ) over a large-field (degrees) at 450μm	0.1mJy (10σ) over a small field (5 arcmin) 0.3 mJy at 850μm 1mJy over fov at 200μm	Number counts may be limited by background confusion
Resolution	<2" at workhorse band	1"	To avoid local confusion limit in crowded distant clusters
Field of view	2x2 arcmin	4x4 arcmin	Wide-field mapping of OB star-forming regions.

3.2.5 The origin of dust: supernovae and evolved stars.

Submillimetre astronomy relies on the existence of interstellar dust, but surprisingly very little is known about its origin. It is generally assumed that about half the dust in the interstellar medium has been produced in supernovae, but there is almost no evidence that this is the case. In the early universe, the problem with the alternative dust formation mechanism – winds from evolved stars – is that these take too long (e.g. Edmunds 2005). There is clear evidence that the Universe was already very dusty even at redshifts of 5 or greater (see section 0).

The ideal way to test this is to observe dust in supernovae remnants which are young enough that little dust will have been swept up from the ISM, but even young supernova remnants are too large and with too low surface brightness to be mapped with current facilities. Only two (Cass A – see Figure 6, and Kepler) are bright enough to even consider mapping at 850μm; however, these data are controversial because of potential confusion with unassociated dust in the line of sight (Krause et al., 2004). Another problem is that the synchrotron emission is significant and dominates the 850μm images (see Figure 7). To help solve these problems would require large-scale mapping at λ~450μm (as well as 850μm) with high spatial resolution to identify the extended dust emission in the SNR.

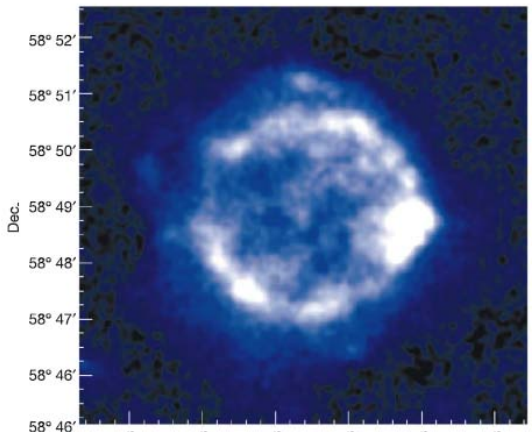

Figure 6: image of Cass A SNR at 850μm (Dunne et al., 2003).. Note that the image is dominated by synchrotron emission (see text for details).

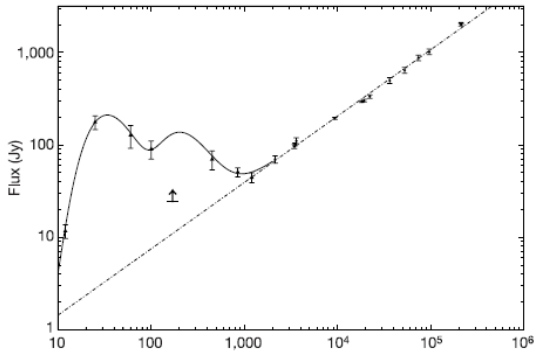

Figure 7: Spectral Energy Distribution from Cass A (Dunne et al., 2003). Only at wavelengths between 100 and 450μm does the emission from cool dust dominate over the synchrotron radiation.

The other potential source of dust – evolved stars – produce extended dust shells that are detected many arcminutes from the parent stars. However, since episodic violent ejection

can produce rings of enhanced emission only a couple of arcseconds thick, *SCELT would be unique in imaging not only the entire shell but also resolving the ring-like features*. High-resolution imaging would trace the inter-ring spacings, and thus show if episodic ejection occurs on regular or random timescales, and (from the ring width and measurements of the expansion velocity) for how long these episodes last. Although dust is produced by such post-main sequence stars, the physics is poorly understood. Are the shells clumpy, for example, with dust formed only in the densest regions? What are the production rates? Does the dust survive as it meets the harsh interstellar environment at the outer boundary of the envelope? High-resolution imaging is the only way to measure the dust masses in small clumps and a wide field plus high sensitivity is necessary to measure the faint tail of dust at the outer edges of these nebulae. SCELT will be ideal for mapping both types of object – and thus answering the question of where and how dust is formed.

Table 7: requirements from dust origin science

Parameter	Requirement	Desirable	Notes
Wavelength	450μm, 850μm	350μm	Shorter wavelengths and spectral slope to discriminate against synchrotron emission.
Sensitivity	1mJy (10σ) at 450μm 0.2mJy (10σ) at 850μm	0.1mJy (10σ)	Extended emission over ~arcminutes, so this is sensitivity when imaging the fov.
Resolution	2” at workhorse band		More detailed structure and comparison with high-resolution synchrotron maps helps discriminate against other dust along line of sight.
Field of view	2x2 arcmin	5x5 arcmin	Wide-field mapping SNRs

3.2.6 Polarisation of dust

Aligned spheroidal dust particles produce at low frequencies very substantial polarised emission. Even when the grains have small elongation (axial ratio ~1.4) the polarisation reaches ~20% and higher values can be observed for more cylindrical dust. The wavelength dependence of the polarisation is flat in the far IR and submm and does not vanish for arbitrarily small optical depths. This is quite contrary to polarisation by dust extinction. If one detects towards a dust cloud polarised submm radiation and simultaneously polarised light at much shorter (optical) wavelength from embedded or background stars, one would notice that the polarisation vectors associated with these two processes, emission and extinction, are perpendicular to each other. The ratio of the submm and visible polarisation provides unique information to constrain the shape of the dust particles. The dust geometry and the elongation parameter of the grains in particular, is directly related to the submm extinction property. Knowledge of the submm extinction is most important as it is widely used to measure the conversion of flux to dust mass. But

with current instruments the relatively low angular resolution and sensitivity, limit sub-mm polarimetry to only the very brightest regions of clouds. Today, star formation regions have been detected with polarisation from ~1% in unresolved central clumps, up to ~20% in the resolved outer regions (see Figure 8).

Figure 8: polarisation of 850μm continuum from the NGC2068 star formation region (Matthews & Wilson, 2000). Y-axis scale is in arcminutes. Complex structure can be seen, frequently unresolved by the beam (14 arcsec), at a high level of polarision (up to 12%).

The fractional polarisation and angle provides *unique* information about the dust alignment, magnetic field structure, and grain structure and elongation that is unavailable at other wavelengths. The extreme sensitivity, angular resolution and wide field of SCELT will allow us to measure polarisations of regions which can currently only just be detected at sub-mm wavelengths. It also provides high spatial resolution to investigate the detailed magnetic field structure.

An example of the use of such an instrument would be to measure the polarisation of debris discs, to investigate dust grain alignment mechanisms within these systems. For the extended disc of ε Eri (Figure 1), the fainter emission is ~8mJy/beam at 850μm, or a few mJy/beam with SCELT at 450μm (assuming extended emission, with some degree of clumpiness). Discs out to distances of ~tens of pc would have similar surface brightness level. For 5% polarisation, this would imply ~0.2mJy polarised flux per beam at 450μm. This would be detected at ~10σ in 10 hours with SCELT.

Table 8: requirements from polarimetry

Parameter	Requirement	Desirable	Notes
Wavelength	450, 850μm (simultaneously)	350μm	850μm is more desirable than 350μm, as polarimetry requires a more stable atmosphere than photometry.
Sensitivity	<0.1mJy (10σ) polarised flux at 850μm	<0.1mJy (10σ) polarised flux at 450μm	
Instrumental polarisation	<1% stable to <0.2%	<0.5% stable to <0.1%	subject to calibration plan
Resolution	<3" at workhorse band	2"	
Field of view	2x2 arcmin	5x5 arcmin	

3.2.7 Completing the census of the Galaxy: a submm galactic plane survey

There is *no* survey of the entire Galactic Plane in the submillimetre continuum (at even the crudest resolution). Currently the best available data are the 8-arcminute resolution maps of optically thick emission from CO molecules (Dame et al., 2000). Since dust is a much better unbiased mass tracer, a submillimetre Galactic Plane survey will give a true census of the star-forming cloud population and the total mass of cold dust in our Galaxy. At the moment, more is known about the dense clouds in Andromeda Galaxy than about those in the Milky Way. In the next few years, surveys with SCUBA-2 on JCMT will trace dust down to several tens of mJy in sections of the plane. But with SCELT a 180 x 2 degree Galactic Plane survey at 450μm to a 1σ depth of 1mJy would take only 30 nights, and would detect and resolve not only the coldest pre-stellar core population but would detect cores down to only a few Jupiter masses at distance of the Galactic Centre. Such a survey with SCUBA-2 on the JCMT is well below the confusion limit of a 15-m telescope and would take many hundreds of years – even if it were possible!

Table 9: requirements from Galactic plane survey science

Parameter	Requirement	Desirable	Notes
Wavelength	450μm	350μm, 850μm	
Sensitivity	10mJy (10σ) at 450μm		Very large-scale mapping (360 sq. degree)
Resolution	<2" at workhorse band		Sets confusion limit in galactic centre and along

			spiral arms.
Field of view	5x5 arcmin	10x10 arcmin	Wide-field mapping, so maximise the number of pixels.

3.2.8 Cold dark matter in Galaxies

The only reliable way to trace the bulk of dust in Galaxies is through submm imaging. It is becoming clear that most of the dust mass in spiral Galaxies lies in extremely cold, low-surface brightness disks, often extended far from the galactic nucleus. Submm spectral energy distributions show dust temperatures around 10-20K (Siebenmorgen et al., 1999; Stevens et al., 2005).

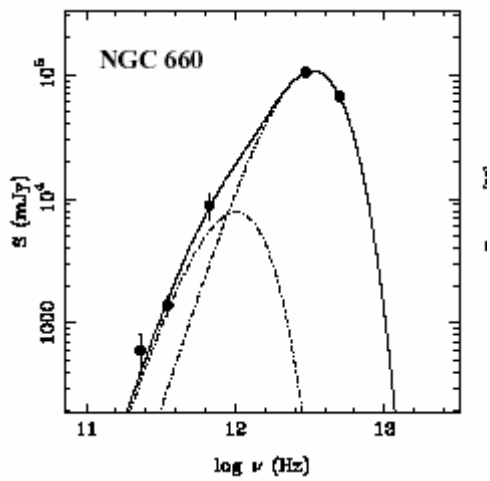

Figure 9 Spectral energy distribution of a typical spiral galaxy. Most of the submm emission is from a cold dust component at T~20K (Stevens et al., 2005).

Such cold dust radiates strongly in the submillimetre, but is orders of magnitude fainter in the far-infrared (Figure 9). Understanding this component is critically important, as it dominates the total dust mass. How far it extends beyond the stellar disc and the relationship to the Galactic ISM is unknown. How much this cold material contributes to the total mass at large radii, and hence how it affects the rotation curve is also unclear. In terms of studying this material in the Local Universe, 2 arcsec at z ~ 0.1 (distance of ~500Mpc) corresponds to a resolution of 5kpc and a survey of cold dust would resolve a population of galaxies to z ~ 0.1 – around the limit of the all-sky Schmidt surveys.

Furthermore, the imaging power and resolution achievable with SCELT would allow the study of individual giant molecular clouds far from the galactic nucleus in nearby galaxies. This would address unique issues such as whether molecular cloud-cloud shielding or high HI optical depth can result in substantial underestimates of the gas surface density, and hence seriously compromising optical studies of star formation efficiency. In addition to studying individual nearby galaxies, SCELT will be vital for determining the low-z benchmarks, such as the local luminosity and dust mass functions, which are needed to interpret information from the deep cosmological surveys. This requires mapping of

substantial portions of the sky, but poor resolution and sensitivity have hampered surveys of this kind with IRAS and subsequent missions.

Understanding the mass distribution of interacting Galaxies is important, as this may be the way that Galaxies formed in the early Universe. SCELT will be a vital tool to map cool dust in interactions in the local universe (out to distance of 500Mpc).

Specific questions to answer are:

- How is the cold dust distributed in nearby Galaxies? Does it extend beyond the warm dust or star forming disc?
- How much does the cold component contribute to the dark matter content?
- How do Galaxies interact? Is there a significant cold dust/gas component we are currently missing in interacting galaxies?

Table 10: requirements from cold dark matter science

Parameter	Requirement	Desirable	Notes
Wavelength	350μm 450μm	850μm 200μm	To get SED
Sensitivity	1mJy (10σ) at 450/350μm	0.1mJy at 850μm 3mJy at 200μm	
Resolution	<2" at workhorse band		
Field of view	2x2 arcmin	5x5 arcmin	Mapping of nearby spirals and interactions

3.2.9 Intergalactic medium

Galaxy Clusters with massive central Ellipticals have a hot extended X-ray halo, often many arcmin across in the closer objects. This was originally thought to be a cooling flow, and is likely linked to dark-matter haloes. In many cases this emission is thought to have a significant and possibly extended *cold* component; gas has been observed using CO in some of the brightest objects (e.g. Edge, 2001) and in HI (see Figure 10). However the masses are extremely uncertain, and in most cases, the dust is somewhat underabundant and therefore too weak to detect – let alone map – with existing instrumentation. But it is not clear whether this cold material is linked to possible mergers, rather than the cooling flow.

How significant is the mass of this cold component? Is it primordial? What is its' metal content? What is its' distribution compared with the X-ray observations? These can be answered by deep extended mapping of in the sub-mm continuum, looking for the cold dust component. The resolution must be sufficient to separate out the Galaxies themselves,

leaving only extended dust. This is a project ideally suited to the high mapping sensitivity and fov of SCELT.

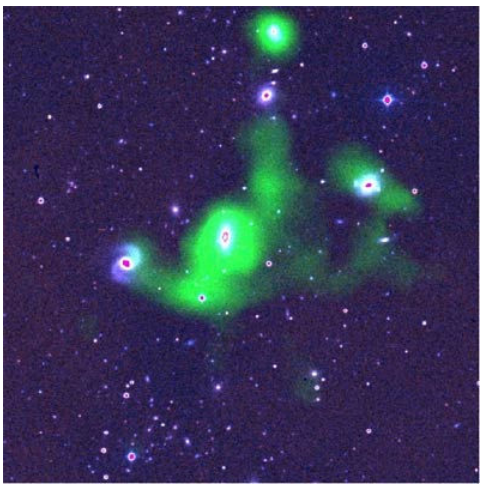

Figure 10: A Hickson Compact Group of galaxies, with (in green) distribution of cool HI. Streamers of HI can be seen linking the galaxies, and the mass of this material may dominate the cool mass in the system (Yun et al., 2006). These fields are ideally suited to the SCELT fov.

3.2.10 Galaxy formation

The negative K-correction for dust emission in the sub-mm passband (Blain & Longair 1993) means that an extremely luminous, dusty starburst with bolometric luminosity of 10^{13}Lsolar would have an 850μm flux of ~10 mJy (within a factor of ~2) if observed at *any* redshift between 1 and 10. Hence the sub-mm provides access to the Universe at epochs as early as only 5% of its present age. This is illustrated in Figure 12, which shows the SED of M82, a nearby luminous galaxy, at various redshifts.

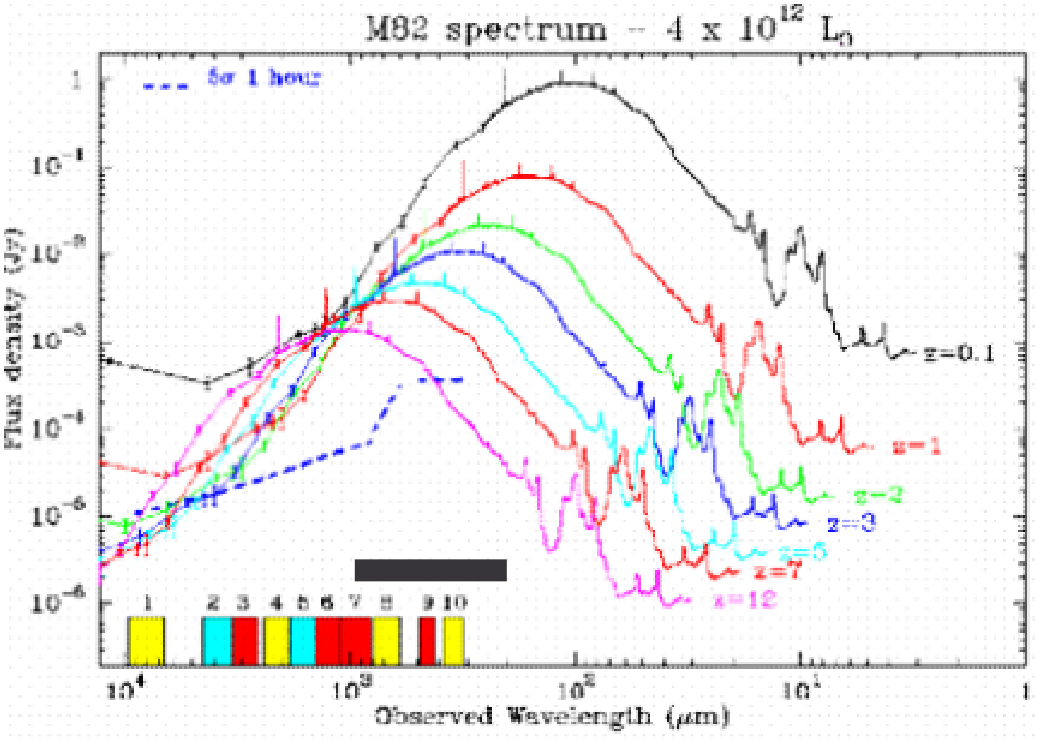

Figure 11: Figure 12: Spectral energy distribution of M82 observed at various redshifts. The key wavelength range of SCELT is indicated by the black bar

At wavelengths other than the sub-mm, the effects of cosmological dimming mean that it rapidly becomes extremely difficult to detect ever more distant galaxies, and it can prove virtually impossible to determine whether or not galaxies do actually exist at extreme redshift z > 5. Unbiased surveys of various sizes and depths – the "wedding cake" approach – are crucial for studying the formation and evolution of galaxies. Although SCUBA has radically changed our view of early star formation, current surveys have only uncovered a few hundred submm-selected galaxies. During the next decade instruments such as SCUBA-2 on JCMT will extend this to more statistically reliable samples. However, the confusion limit for 15m-class telescopes means that such surveys can only detect the most extreme objects – rare, massive galaxies forming over 1000 solar masses of stars every year in the early Universe (z>3). SCELT would not only give a vast increase in mapping speed over any other planned facility, but would be able to probe and importantly find new objects down to much lower star formation rates than current single-dish telescopes. For example, a $1L_*$ galaxy at z=3 would have an 850μm flux of 10-100μJy, easily detectable with SCELT. Unbiased samples of galaxies of all types and luminosities could therefore be assembled very rapidly. Moreover, to probe the evolution of more normal galaxies, such as the U, B and V-dropouts that are believed to be the precursors of modern-day disk galaxies, it is necessary to probe below the present confusion limit to few tens of μJy. This could be achieved with SCELT in only a few hours.

SCELT will therefore give us the unique ability to detect galaxies with star formation rates similar to the Milky Way throughout the Universe.

3.2.10.1 Imaging the Universe in 3-D

The ability to simultaneously measure the submm fluxes provides a method of estimating the redshift to within ±0.4 or better (e.g. Hughes et al., 2002). This can be seen in the differences in sub-mm curvature of the template SEDs in Figure 12; it is not possible to do this at λ>1mm except for redshifts ≥20. Furthermore the severe confusion limit with the small apertures of far-IR satellites causes problems with cross-identification of objects at multiple wavelengths. Indeed in the absence of extremely deep infrared/optical or time-consuming sub-mm spectroscopic searches, sub-mm photometry at high angular resolution may be the *only* way to constrain z of a large number of galaxies.

The deep widefield imaging capability of SCELT at multiple wavelengths will provide photometric redshifts, giving us a 3-D view of the distant Universe.

Table 11: requirements from Galaxy formation science

Parameter	Requirement	Desirable	Notes
Wavelength	850μm, 450μm	350μm	Shortest wavelength does not have K-correction advantage at z>5. But can be used to constrain redshift.
Sensitivity	0.1mJy (10σ) at 450μm 0.03mJy (10σ) at 850μm	0.03mJy (10σ) at 450μm Reaching 1σ/ 1beam confusion limit.	Sensitivity whilst imaging a single field-of-view.
Resolution	<2" at workhorse band		To provide lowest confusion limit
Field of view	5x5 arcmin	10x10 arcmin	

3.2.11 Large-scale clustering

The ensemble of existing extragalactic surveys with SCUBA have successfully resolved the bulk of the submillimetre background (e.g. Blain et al., 1999), established the importance of dust-obscured star formation in the early Universe, and investigated the clustering of the most active galaxies on scales up to 1Mpc. Attention has now shifted to the fundamental nature of submillimetre galaxies and their role in the history of structure formation: do bright submillimetre sources really represent forming ellipticals, or merely short-lived bursts of violent activity in the progenitors of more modest galaxies? What is their relationship, if any, with high-redshift optically selected galaxies? Wide-field surveys with sensitivities well below the current confusion limit are required to address these issues. If bright submillimetre galaxies are indeed the progenitors of massive ellipticals then they should be strongly clustered, with scale lengths of around 10Mpc (roughly 30 arcmin). A survey covering 10-100 square degrees with a rms sensitivity of a few hundred

μJy is thus required, and this can *only* be done with SCELT. Such a survey would detect many less luminous galaxies (currently selected only in the optical), allowing their clustering to be properly assessed, unbiased by obscuration, and compared with modern-day galaxy populations. Since massive ellipticals dominate the cores of rich galaxy clusters, such surveys will provide an important tracer of the growth of large-scale structure in the very early universe.

Table 12: Requirements from clustering

Parameter	Requirement	Desirable	Notes
Wavelength	850μm, 450μm	350μm	Shorter wavelengths can be used to constrain redshift.
Sensitivity	1mJy (10σ) over 10 sq. degrees at 450μm	1mJy (10σ) over 100 sq. degrees	At 850μm or 450μm
Resolution	2" at workhorse band	<2"	

3.2.12 Cosmic star-formation history.

It is known from studies of the Cosmic Microwave Background that the universe started off in a very uniform state, with no real structure. At some point the "Cosmic Dark Ages" came to an end through the birth of the first stars within primordial galaxies. Nuclear energy was converted to light in stellar interiors, and had important heating and ionisation effects on the surrounding medium. Exactly how this process began and subsequently evolved is one of the greatest cosmological puzzles. Recent work in the submillimetre has shown that luminous infrared galaxies evolve more strongly than their more normal optically-bright counterparts. It has also become clear that luminous obscured galaxies at high redshift contribute a substantial fraction (arguably the majority) of the total emitted radiation in the Universe. Roughly half of all the stars that have formed by the present day have probably formed in highly obscured systems. To trace the star-formation history of the various classical galaxy types (ellipticals, spirals) over cosmic history with sufficient precision would require a sample size of around 1 million galaxies. A large project such as this would require mapping 10 sq. degrees to 0.02mJy (1σ) sensitivity at 850μm; this could be achieved in a few weeks observing with ELT. The high spatial resolution would yield accurate galaxy positions, whilst simultaneous 850 and 450μm measurements (and preferably also 350μm of the brightest) would allow photometric redshifts to be obtained.

Table 13: requirements from cosmic star formation science

Parameter	Requirement	Desirable	Notes
Wavelength	450μm, 850μm,	350μm	Multi-wavelength to get redshift
Sensitivity	0.2mJy (10σ) at 850μm	0.2mJy (10σ) at 450μm	Over 10sq.degrees
Resolution	2" at workhorse band		
Field of view	5x5 arcmin	10x10 arcmin	Larger is better

4 Final summary specifications

Parameter	Requirement	Desirable	Notes
Wavelength	450μm 350μm (simultaneously)	850μm (possibly 200μm)	200μm is lower priority than 850μm because of relative insensitivity of this band (see 5.1)
Sensitivity	450/350μm: <1mJy (10σ)	450/350μm: <0.3mJy (10σ)	10σ, 1hr, point source (mapping fov of array)
	850μm: <1mJy (10σ)	850μm: <0.3mJy (10σ)	10σ, 1hr, point source
	200μm: 10mJy (10σ)	200μm: 2mJy (10σ)	10σ, 1hr
Resolution	<4" at workhorse bands	2"	
Field of view	5x5 arcmin	10x10 arcmin	
Number of pixels		850μm: 15,000	Numbers represent fully-filled fov (5x5 arcmin) with detectors Nyquist-sampling the sky at each wavelength.
	450μm: 50,000	50,000	
	350μm: 85,000	85,000	
		200μm: 250,000	
PSF accuracy	PSF can be calibrated (i.e. is stable) to better than 1% of central peak out to 10 arcsec radius.	Same calibration accuracy within 20 arcsec	Avoiding confusion from bright sources
	PSF sidelobes are <0.1% at >10 arcsec radius		
Observing modes	Fully-sampled mapping of array field of view. Scan-mapping (areas of >10 sq. arcmin to >100 square degrees).	Hitchhiker mode, with simultaneous sub-mm and optical or infrared observing	
Calibration accuracy	<10% at all wavelengths	<5% at all wavelengths	Relative to standard sub-mm sources, such as planets/asteroids.
Polarimetry	IP<1%	IP<0.1%	

5 Detailed Best Effort Calculations of Performance

The performance of the baseline SCELT design is based on the following assumptions.

Parameter	Value	Notes
Telescope aperture	42m	Need to scale for a 30m primary
Central obscuration	5m	
Primary mirror segment gaps	5mm	Sees warm telescope between gaps. Segment diameter=2m
Telescope effective radiation temperature	275K	
Pixel coverage of field of view	100% at all wavelengths	Fraction of science field of view that is covered by Nyquist-sampled pixels
Precipitable water vapour content	0.5mm (for 850, 450, 350μm) 0.2mm (for 200μm)	See 8.2
Airmass	1.2	Elevation 60 degrees
Atmospheric model		Uses transmission curves from Hitran model, updated 2003
Filter bandwidths	Optimised for atmospheric transmission window	Based on Scuba-2 design
Window losses	4%	Based on Scuba-2. May be thicker, so larger losses for SCELT
Filter losses	5%	Filters at 1K
Cold stop temperatures	1K	
Dichroic losses	5%	Dichroic at 1K.
Detector NEP	$<1.5\times10^{-17}$ W/√Hz at 450 & 350μm $<3\times10^{-17}$ W/√Hz at 850μm $<8\times10^{-17}$ W/√Hz at 200μm	<1/2 of background power
Detector temperature	<100mK	

5.1 Summary of performance

Wavelength	850µm	450µm	350µm	200µm	Units
Resolution	5.0	2.6	2.1	1.2	FWHM, arcsec
System NEFD [1]	1.8	3.8	6.4	~10 [1]	mJy/√Hz
Per pixel sensitivity [2] (10σ, 1hr)	0.3	0.6	1.1	2 [1]	mJy
Confusion limit (1σ, 1beam) [3]	3	1	1	1	µJy
Large-scale mapping sensitivity [4] (10σ, 1hr, 1 sq.degree)	4	8	13	20	mJy
No. of pixels [5]	15,000	50,000	85,000	250,000	
Pixel spacing [5]	2.5	1.3	1.0	0.6	arcsec
Field of view	5	5	5	5	arcmin
Time to image field of view to detect (at 5σ) 1 background source in 30 beams: "confusion limit" [6]	0.05	0.2	7	>>1000	hours

1. For 0.5mm PWV, airmass 1.2, *except at 200µm*, where we assume 0.2mm pwv
2. Sensitivity reached (10σ, mJy) per pixel on the sky
3. See section 6. Note units in µJy
4. Sensitivity (10σ, mJy) reached in a Nyquist-sampled map of 1 square degree in 1 hour (no overheads included).
5. Assuming arrays covering full (Nyquist) sampling of the field of view. See section 11.1)
6. Commonly accepted limit to avoid confusion-limited observations is 5σ, 30 beams; See section 6

Comparison to Existing and Proposed Facilities and Space Missions

This section compares SCELT with other ground and space-based facilities designed to operate over similar wavelengths, so which are likely to be doing comparable science. The important wavelength regime in this comparison is 200-3000μm, i.e. the Rayleigh-Jeans tail of cool dust at redshifts z<2. Table 14 summarises the features of the main instruments and telescopes, including those existing, under construction, and planned for the next decade. In 6.2 & 6.3 the sensitivities are compared in detail, and in 6.5 the complementarity of SCELT and ALMA is illustrated.

The baseline atmospheric water vapour content (PWV) for the ELT site in this comparison is 0.5mm. We assume a 42m diameter ELT, with a 5x5 arcmin FoV, Nyquist-sampled pixels (ie fully-filling the field of view). We show in sections 8.1.1 and 7.3 comparisons of sensitivity with different ELT diameters (30 or 42m) and PWV, which can be used to scale the other comparisons. The comparisons are based on the parameters in Section 5.1. A detailed spreadsheet for these is available on request.

The following table shows the existing and proposed facilities operating in the submm and far-infrared.

Telescope /aperture	Instrument	λ (μm)	Pixels	Resolution (arcsec)	Sensitivity (10σ/1hr) (mJy)	Date	Notes
JCMT 15m	Scuba	850 450	37 91	14 7	10 70	-2005	
"	Scuba-2	850/450	5100/ 5100	14 7	3 16	2007	
IRAM 30m	Mambo-2	1200	117	10	6	Now	Only at mm wavelength
LMT 50m	Bolocam-2	1100	151	5.5	0.5	2006	Only at mm wavelength
GBT 100m	PenCam	3000	64	7.5	0.02	2008?	Only at 3mm wavelength
Apex 12m	Laboca	870	295	18	2.5	2007	Also ASTE 10m
"	"C2"	350	300	7.2	13	2008?	
ALMA (500-10000)		850 450 350		0.4 – 0.01 (con-figurable)	0.2 2.5 7	2012	Also at λ>1mm
Herschel 3.5m	SPIRE	500 350 250	43 88 139	35 24 17	8 7 5	2008	
Sofia 3.5m	HAWC	200 to 50	384	14" @200μm	30 (at 200μm)	2008	
SPICA 4m	FCS	50-200	>200?	~10	~3?	2012	
CCAT 25m	Cornell-Caltech	850 450 350	20000?	8 4 3	0.5 0.8 1	2012?	Proposed telescope
ELT 42m	**SCELT**	**850 450 350 200**	**15,000 50,000 85,000 250,000**	**5 2.7 2.0 1.2**	**0.3 0.6 1 10**	**2015 ?**	

Table 14: Proposed and existing submm facilities

5.2 Per pixel comparison

First we ignore the fact that SCELT is an array, and look only at the sensitivity of each pixel, assuming an unresolved source.

5.2.1 Flux sensitivity

The charts in Figure 13 compare the sensitivity (NEFD, mJy/√Hz) *per pixel* for current and planned submm cameras at ~850μm and at 450μm. To convert to sensitivity in 10σ/1hr, divide by 6. Note that we have included in the 850μm comparison the IRAM/30m and LMT/50m values; these operate at 1300 and 1100μm, so the effective sensitivity at 850μm would be a factor of ~2 worse (higher NEFD) than the values shown (assuming some reasonable dust emissivity law). The SCELT sensitivity assumes 0.5mm PWV, i.e. a good site.

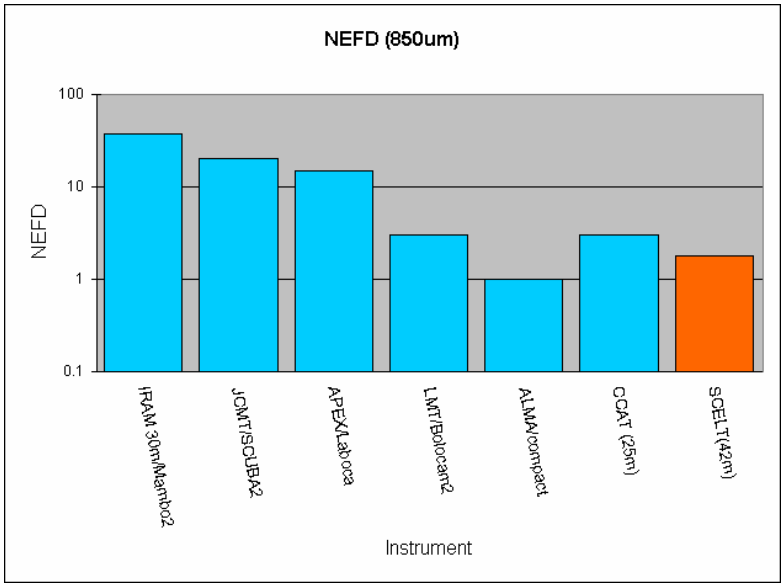

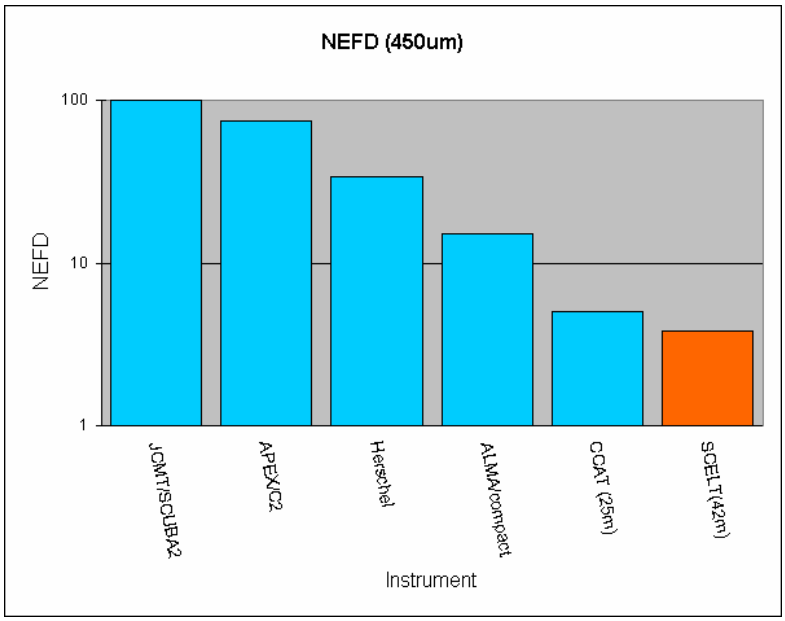

Figure 13: Comparison of sensitivity of *one pixel* of SCELT with other facilities at 850 (top) and 450um (bottom). At 850μm one pixel of SCELT is comparable to the ALMA sensitivity, but at 450μm one SCELT pixel is considerably better than ALMA.

The results show that SCELT on a 42m ELT (shown in orange) will be similar in sensitivity *per pixel* to ALMA and CCAT at 850μm. At 450μm SCELT has a factor of 4 advantage because of the better sensitivity of the bolometers and improved assumed site characteristics.

5.2.2 Dust mass sensitivity

Much of the science with SCELT will be carried out by observing dust in the nearby Universe. With this assumption, we can do a comparison of sensitivities at different wavelengths. For dust at T>30K at z<2, the emission has a spectral index slope of ~2+β, where β=0 (for pure black-body) to 2.0 (for small ISM grains). Taking β=1, Figure 14 shows the relative gain of SCELT (using a 42m ELT, shown in orange) for a given *mass* of dust, compared with other facilities. The scale is relative to SCUBA on JCMT at 850μm. Where there are two bars for one instrument, this shows the gains at different wavelengths; in the case of ALMA, LSD and SCELT the wavelengths shown are 850 and 450μm.

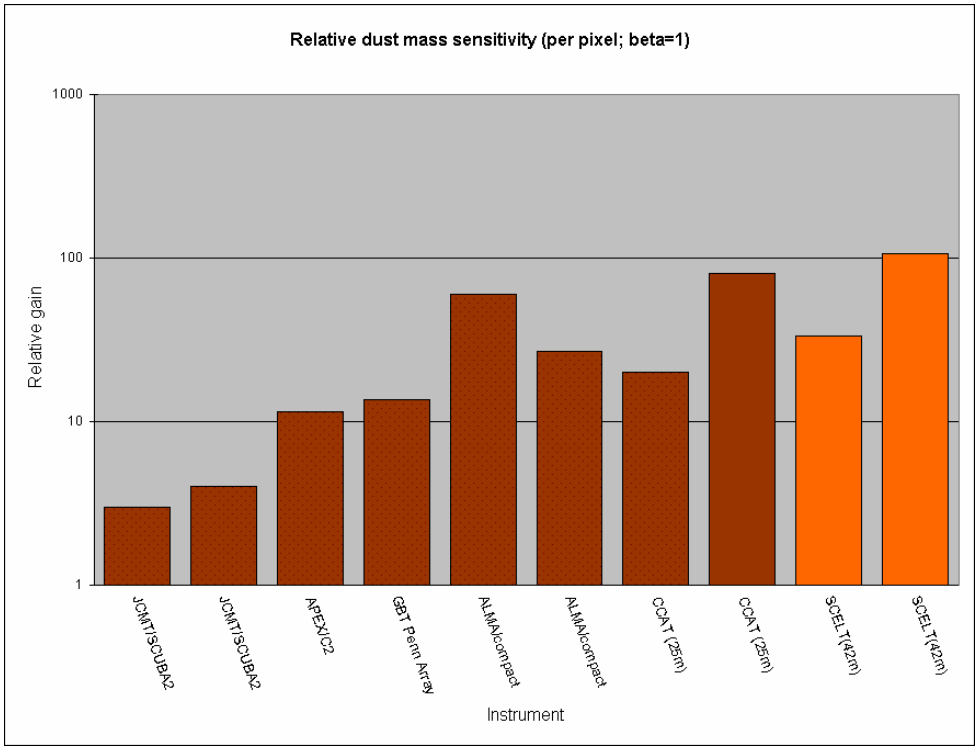

Figure 14: Relative sensitivity of facilities to a given mass of warm dust, *per pixel*. SCELT is shown in orange; where two values are given, the rightmost one is the shorter wavelength (450μm) and the left is 850μm.

Figure 14 indicates that SCELT operating at 450μm on a 42m ELT will be ~30 times more sensitive, *per pixel*, to a given mass of dust compared with SCUBA-2. Even compared with ALMA, SCELT will be 2x more sensitive to a given dust mass at the shorter wavelengths. Note that these gains are per pixel - there are 20,000-100,000 pixels in SCELT.

5.3 Mapping comparison

The area where SCELT provides the most gain over future projects like ALMA comes from the massive multiplex advantage of the large focal plane. The mapping speed, i.e. time to map a fixed area of the sky to a certain depth, depends on the number of pixels and beamsize, as well as per pixel sensitivity. Figure 15 below compares the relative mapping speed of various facilities at 850 and 450μm.

- SCELT will be ~1000 times faster in mapping at 450μm compared with the state-of-the-art instrument, SCUBA-2.
- Large-scale mapping projects will clearly be more suited to focal-plane arrays such as SCELT than interferometers like ALMA; *the SCELT mapping speed will be at least 10^5 times faster than the best (ie compact) ALMA configuration.*

The smaller beam size of SCELT on a 42m compared with other single-dish telescopes gives it another key capability – a lower confusion limit. This is described in the next section.

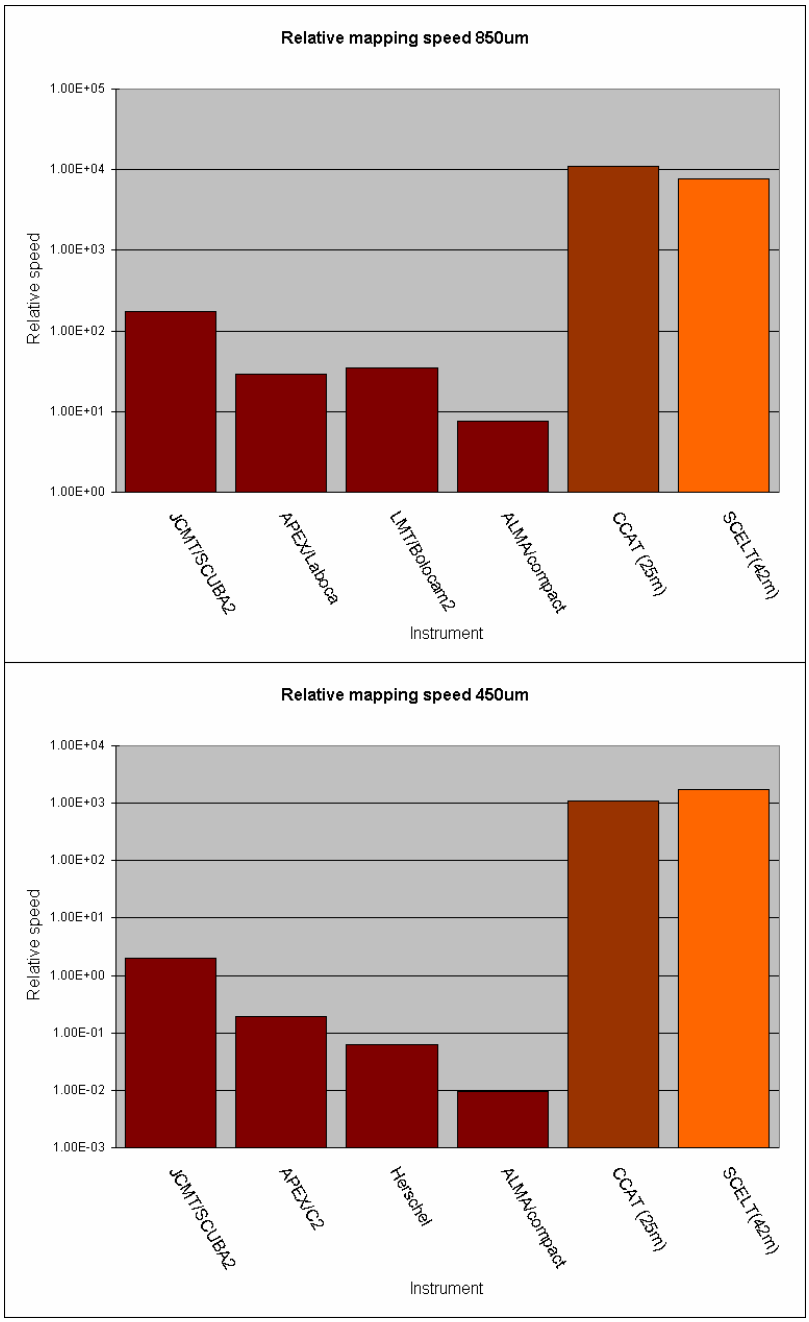

Figure 15: Relative mapping speed at 850 and 450μm. This shows the relative time for different instruments to map a certain area on the sky to a fixed depth. Large-format focal plane arrays such as SCELT fare well in this comparison[2]

[2] SCUBA-2 and LMT/Bolocam2 score relatively highly in this chart purely because they have relatively low resolution or operate at a longer wavelength (1.1mm) and so are relatively sensitive in mJy units.

6 Confusion limits

The sub-mm sky is full of sources. Source confusion for sub-mm and far-infrared telescopes will limit the ultimate point-source sensitivity; in cases where the target source is compact with a known position this can be expressed as the 1σ/1beam sensitivity. For other projects, the number of bright confusing sources over the mapping area will limit the ability to measure, for example, the number density of nearby faint objects in a galactic cluster. Sources of confusion include:

- Solar System Zodiacal dust. This dust is warm (~200K) so is only significant in the mid-IR.
- Galactic cirrus. Cool (~22K) so important in submm. Concentrated towards Galactic Plane.
- Galactic star formation regions. Only dominates in certain regions of the sky.
- High redshift galaxies. Isotropic.

Confusion from high-redshift objects and Galactic cirrus are potentially the most significant problem for the submm. The importance of these is estimated below.

6.1 High-redshift objects

The potential problem with the extragalactic background and advantages of smaller beams are illustrated in Figure 16, where models of the confusion limit of SCUBA-2 on JCMT are compared with those of SCELT.

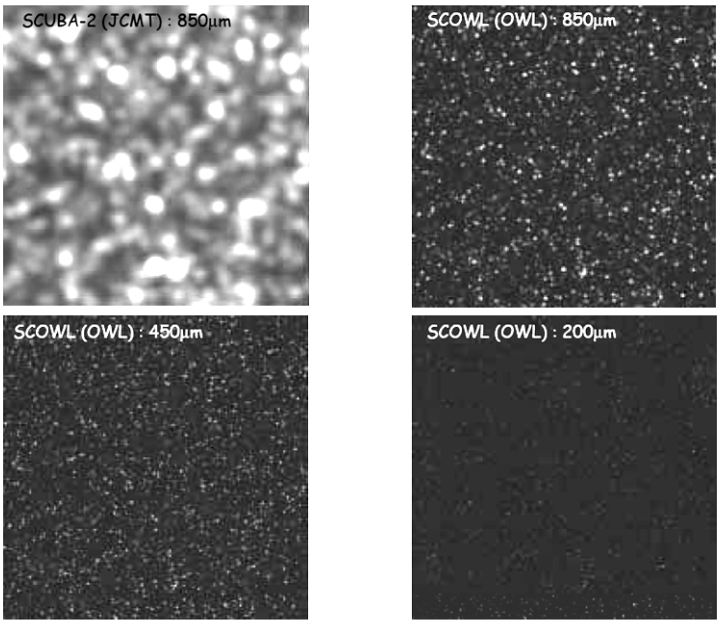

Figure 16: Representations of confusion limited surveys of a 0.2 deg2 area of sky for JCMT/SCUBA-2 at 850μm and ELT/SCELT at 200, 450 and 850μm. Based on the models of Hughes and Gaztanaga (2000), with simulations carried out by Ed Chapin (details in Chapin et al.) 2002). Note that this simulation was originally for a 100m OWL telescope, so the resolution of ELT will be ~2-3x lower than shown.

To estimate the all-sky background confusion limit, we have used the models of Pearson (2001, 2005)[3] and Rowan-Robinson (2001), which use different galaxy evolution models. A comparison of the two is given in Table 15. Note that these are extremely uncertain, particularly at the shorter wavelengths, and depend on the populations and evolution of different objects at high redshifts, but recent source counts have not changed the values significantly, and tend to confirm the Pearson 450μm base level (e.g. Greve et al., 2004).

Table 15: Confusion limit from background sources for a 42m ELT. Limits are 5σ, 40 beams, in mJy.

Wavelength	850μm	450μm	350μm	200μm
Pearson (2005)	0.51	0.17	0.097	0.018
Rowan-Robinson (2001)	0.78	0.93	0.68	0.023

[3] Available on the web at http://www.ir.isas.jaxa.jp/~cpp/research/counts/

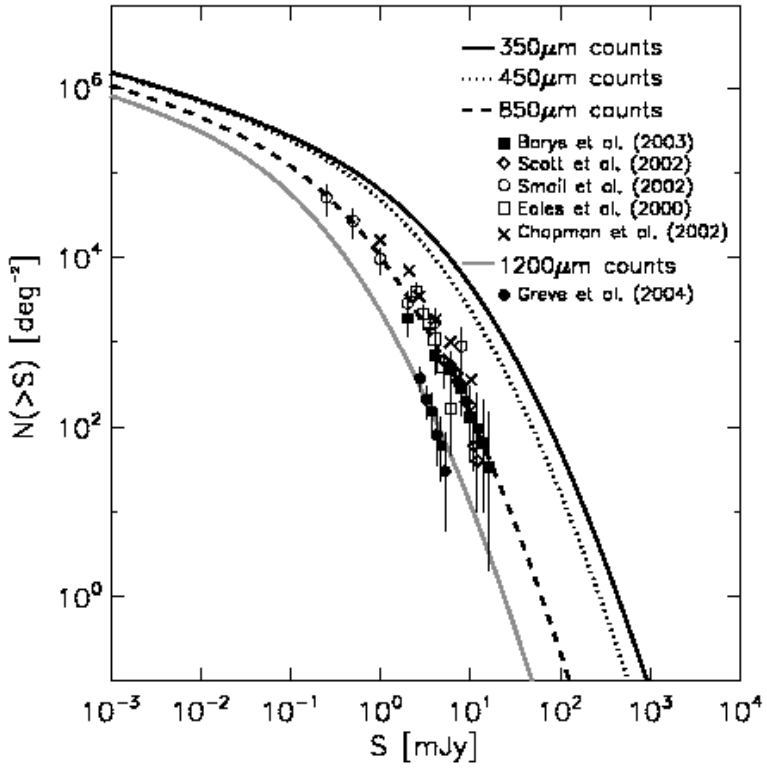

Figure 17: Background number counts at submm and mm (based on models of Pearson (2001) and T. Greve, priv. comm.) The plots have been extrapolated to lower flux densities based on galaxy evolution models, but are extremely uncertain.

6.2 Galactic cirrus

This is illustrated by the COBE 240μm map shown in Figure 18. Most of the emission in this figure is cool Galactic rather than hot Zodiacal dust. To estimate the level at longer wavelength we use a mean cirrus temperature of ~22K, with an opacity index 2; this implies the ratio of 240:450 and 240:850 μm fluxes are ~5 and ~40. The fluctuations in background have been measured on the arcsmin scale, not on the 1 arcsec scale. However, if we assume that the approximation for the fluctuations given by Helou & Beichman (1990) are valid down to arcsec scale, then we can derive the confusion levels in the last column of

Table 16. Note that these numbers are highly uncertain, as the small-scale cirrus structure is unknown. It may be that the power in the small-scale structure is a larger fraction of the background level, which will increase these confusion limits.

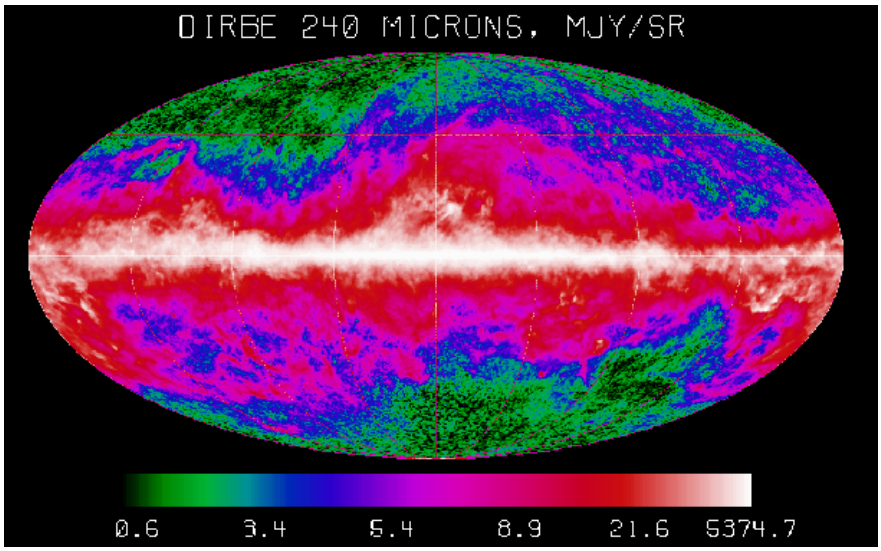

Figure 18. COBE/DIRBE all-sky image at 240μm, showing mainly Galactic cirrus at this wavelength.

Table 16: confusion limits due to Galactic cirrus for different sky coverages. Critical numbers are highlighted.

Wavelength	Fraction of sky not available	Sky brightness level (MJy/str)	Brightness level per beam (mJy/beam)	Confusion level (mJy/beam)
850μm	1%	1.2	≤0.6	0.3
	10%	0.07	≤0.03	**0.02**
450μm	1%	10	≤1.3	0.6
	10%	0.5	≤0.07	**0.04**
350μm	1%	22	≤1.8	0.9
	10%	1.2	≤0.1	**0.05**
200μm	1%	55	≤1.5	0.8
	10%	3	≤0.08	**0.04**

Note to table: (1) the fraction of the sky at or below a certain brightness level at 240μm is taken from Jeong et al., (2005), converted from their 160μm plot with the dust parameters given above.

6.2.1 Confusion-limited observations with SCELT

Comparison of the results in Table 15 and Table 16 shows that background galaxy confusion is dominant over 90% of the sky, and so will set the confusion limit in most general cases. Confusion affects typical observations in three ways:

- The 1σ/1beam confusion limits sets the lowest achievable noise level in a map. It is the lowest flux detectable for a point source of known position.
- An alternative way of expressing the confusion limit sometimes used is 1/30 or 1/40 sources per beam. (eg Takeuchi & Ishii, 2004). This requires that a field of view of 30 beams has no more than 1 significant detection, say at ≥5σ. This is arbitrary, but would result in the detected confusing sources being ~5 beams separated. Worst-case values are given in Table 17 (based on the highest model). For the 850μm beam this is roughly equal to 1 per 100 sq.arcsec. This limit is more appropriate to small-scale mapping.
- For large-scale mapping of point sources, the statistical uncertainty in number of background objects (nominally √N, but probably a factor of ~2-3 higher[4] because of background clustering and lensing) sets a limit to the measurable number density of foreground objects.

The corresponding values for different telescope diameters are given in 8.1.2.

Other methods of differentiating against background sources can be employed:

- Multi-colour imaging, looking at differences in the 350/450/850μm relative fluxes between different classes of objects.
- Proper motion of the foreground objects. This would be useful in nearby stars, within ~20pc, and so would be useful for example in detecting faint clumps in nearby debris discs.
- For large-scale mapping of extended emission, it will be possible to remove bright background *point* sources using post processing. However, it is likely that some background Galaxies will be extended. These may be mostly the more luminous and less common ones.

Table 17: summary of worst case confusion limits for SCELT.

	850μm	**450μm**	**350μm**	**200μm**
5σ/40beam confusion limit: **90% sky coverage**	0.5	0.2	0.1	0.02
Time to confusion limit (for point source) (minutes)	5 minutes	150 minutes	1700 minutes	1000 days

In summary, the confusion limit is likely to be a more serious problem at 850μm, where the beam size is larger and the source count still high. At 450μm and shorter, the confusion limit is lower, yet the source fluxes will be higher (for normal grey-body dust emission from objects at Z<10). This points to a significant advantage for SCELT operation at shorter wavelengths.

[4] Rough estimate, depending on mapping area compared with typical cluster size and enhancement, and lensing effects. Neither of these is currently well known.

7 SCELT and ALMA

7.1 Direct comparison

A wideband sub-millimetre bolometer array on the ELT offers the opportunity to observe a very large field of view with a near perfect dish surface accuracy and a single aperture. Although the premier facility for *high-resolution* millimetre astronomy in the next decade will be ALMA, SCELT will provide a facility which would feed targets into ALMA for high-resolution follow up. However, it would also surpass ALMA in several respects. The larger effective collecting area combined with the wider bandwidth of such a bolometer system will mean a factor of ~4 improvement in point-source sensitivity at 450μm (or x7 at 350μm) (see table below). But clearly the most significant gain will be in the large-scale mapping speed. Table 18 indicates that projects to make extremely deep maps of *square degrees* of sky now become feasible with SCELT; this shows the time to map 1 square degree to a 10σ sensitivity of 0.1mJy. For comparison, the long-term SCUBA-2 legacy large-area survey is planning on mapping a few square degrees to 10σ=7mJy over the next 4-6 years (but with a 14 arcsec beam). Clearly this sort of large-scale project would not be possible with ALMA.

	SCELT (42m)		**ALMA**	
	850μm	450μm	850μm	450μm
Flux sensitivity (μJy, 10σ 1hr)	**300**	**600**	170	2500
Resolution (arcsec)	5.0	2.6	**0.02**	**0.01**
Confusion limit (μJy)	500	200	**<0.4** [5]	**<0.02**
Field of view	**5 arcmin**	**5 arcmin**	20 arcsec [6]	10 arcsec [6]
Mapping speed (time per square degree to a limit of 10σ=0.1mJy)	**100 nights** [7]	**480 nights**	400 *yr*	200,000 *yr*

Table 18: SCELT and ALMA capabilities. Areas where the facility is optimally suited are indicated in red bold.

[5] Worst case, for compact configuration
[6] primary beam
[7] assuming 12-hour nights

7.2 SCELT as a complement to ALMA

Current single-dish facilities have typical resolutions of ≥10 arcsec, compared with ALMA resolution which will be ~100 times higher (see Table 14). SCELT, with its' resolution of ~2 arcsec, neatly bridges the gap. It would, for example, avoid the potential difficulty of locating faint objects in the ALMA primary beam which have been discovered with a small single-dish telescope.

A further advantage of SCELT is that it will detect *all* flux from objects, independent of their size. Interferometers such as ALMA, however, are not sensitive to large-scale structure. Although ALMA will have a compact array of smaller (7m) antennae (ACA), this has a collecting area 12 times smaller than the full system and would be correspondingly less sensitive. So ALMA would resolve out structure larger than ~15 arcseconds at 850μm. Large-scale faint structures in Molecular clouds, or in Galaxy Clusters would not be seen by ALMA alone. But combining SCELT and ALMA data would extend the sensitivity out to structure extended over 5 arcminutes or more. Thus ALMA and SCELT together will provide a uniquely-powerful facility, detecting structure from a few tens of milliarcseconds up to degrees.

Finally SCELT will excel as an instrument to find targets for higher resolution observations. For example, in a single deep integration (4 hours), SCELT will detect ~1000 high-z objects in the fov (see Figure 17), giving a wealth of targets for followup at higher resolution, or at different wavelengths.

In summary, astronomers with access to SCELT as well as ALMA will have a unique advantage over other ALMA users. The importance of such complementarity of the two facilities strongly suggests that ELT should be on a site with a similar latitude to ALMA.

8 Observatory requirements

8.1 Primary diameter: 42 or 30m?

8.1.1 Comparison of sensitivity with different telescope diameters

The two primary *telescope* parameters which will have a direct effect on the SCELT sensitivity are the primary diameter and the atmospheric precipitable water vapour content (PWV – see above). The following shows the effect of primary diameter on the NEFD. This scales the above sensitivity comparison charts.

Note that the atmospheric values shown are at elevation 60^{o} (Airmass 1.2). Observing at an airmass of 2.0 is approximately equivalent to doubling the PWV.

Diameter	NEFD 850μm	NEFD 450μm	NEFD 350μm
42m	1.8	3.8	6.4
30m	3.4	7.3	12.2

8.1.2 Comparison of confusion limit with different telescope diameters

The table below gives the confusion limits and time to reach that sensitivity for SCELT at 850 and 450μm with 2 different telescope diameters, and a comparison with the JCMT. At low flux levels (tens of μJy – see above) the confusion flux level from high-redshift background galaxies depends on the beam area $A^{-2.5}$, or telescope diameter $D^{-4.5}$, whereas cirrus confusion depends on $D^{-2.5}$. The background number counts turn over around 1mJy. We have assumed that 99% of sky coverage is required (giving the larger confusion limits at 350 and 450μm). The final row gives the confusion limit on the JCMT, with SCUBA-2 sensitivities. Note tat these numbers are extremely uncertain, and rely on extrapolations significantly outside the existing measurements.

Table 19: confusion limits for SCELT with various telescope apertures.

Telescope diameter (m)	**Confusion limit (5σ 40-beam, mJy)**		**Time to confusion limit** [8]	
	850μm	450μm	850μm	450μm
42	0.5	0.2	5 mins	2hrs
30	0.9	0.4	5 mins	2hrs
15 (JCMT)	2.4	4.5	1 min [9]	10 min [9]

[8] Note this is time to *avoid* reaching the confusion limit. Often quoted is the time to reach 1σ/1beam confusion, which will of course be much longer than the above.
[9] Assuming SCUBA-2 sensitivities

This table shows that the confusion limit *at 850μm* on a 30m ELT is only a factor of 2-3 times lower compared with the JCMT; this means the available science for faint objects is not significantly improved.

At 450μm the confusion is an order of magnitude lower, and so the improvement over existing confusion-limited science will be very significant.

The limit for a 42m ELT is another factor of 2 better.

8.1.3 Summary

Building SCELT on a 42m telescope rather than a 30m ELT has the following advantages:

- Sensitivity will be 2x better (4x shorter integration times)
- background confusion limit will be ~2x lower
- discrimination against nearby bright objects 2x better

8.2 Requirements for Precipitable Water Vapour and atmospheric transmission

SCELT is pushing towards shorter submillimeter wavelengths, for reasons of uniqueness, sensitivity, confusion and science. Because of this, the choice of site is probably the most important constraint set by SCELT on the ELT observatory. The transmission of the atmosphere in the submm is shown below.

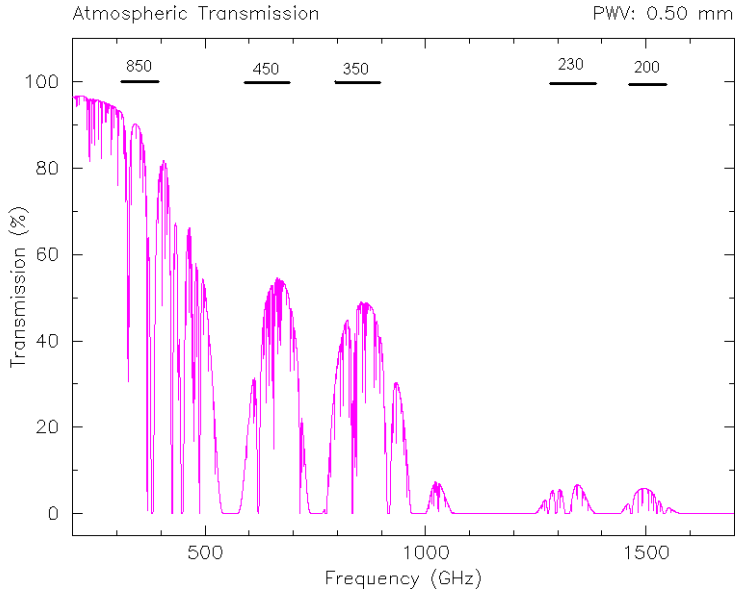

Figure 19: Zenith atmospheric transmission for 0.5mm pwv. The primary submillimetre windows are shown.

The atmospheric transmission at sub-millimetre wavelengths is strongly dependent on the Precipitable Water Vapour content (PWV), and is broken into wavebands determined by the strong water lines. The following figure compares the sub-millimetre transmission for different values of PWV, at 0.1, 0.2, 0.4, 0.8, 1.6 and 3.2mm.

In summary these plots show that:

- The windows at 450μm (670GHz), 350μm (860GHz) have good transmission for PWV<0.8mm. Both have similar transmission characteristics.
- The shorter windows, at 230μm (1300GHz) and 200μm (1500GHz) are usable for PWV<0.2mm.
- The longer wavelength window at 850μm (350GHz) is usable for PWV<2mm.

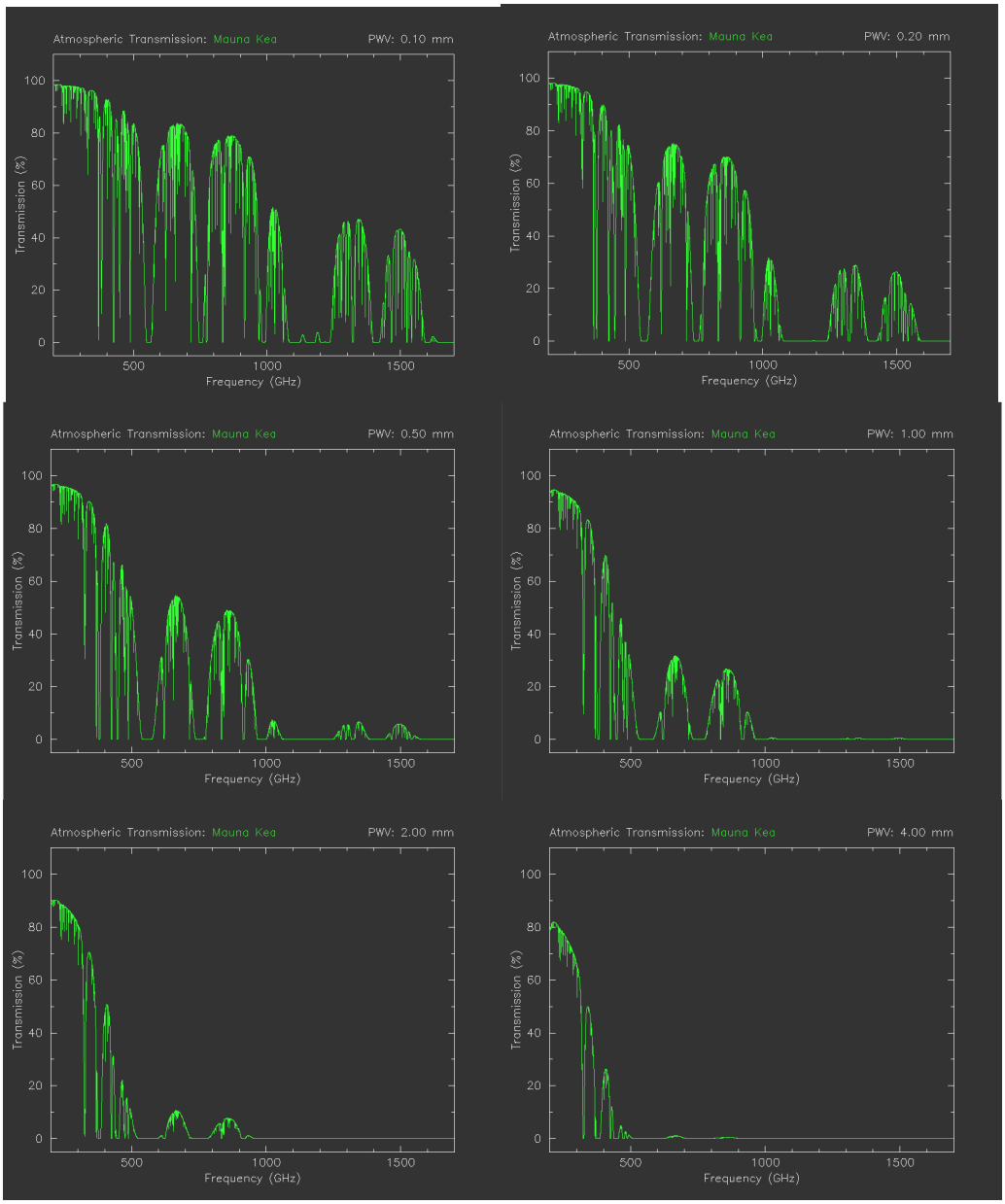

Figure 20: Submm atmospheric transmission for different values of precipitable water vapour, from 0.1mm (top left) to 4mm (bottom right).

8.3 Site and PWV

The atmospheric precipitable water vapour content as described above has a strong effect on the SCELT sensitivity, as shown in the following table.

Note that these sensitivity values shown are at elevation 60^{o} (Airmass 1.2). Observing at an airmass of 2.0 is approximately equivalent to doubling the PWV from Zenith.

Table 20: sensitivity vs. pwv

PWV content (mm)	Optical depth at zenith at 225GHz	NEFD 850µm	NEFD 450µm	NEFD 350µm	NEFD 200µm
0.2mm	τ_{225}=0.02	1.6	2.4	4.0	~10
0.5mm	τ_{225}=0.03	1.8	3.8	6.4	40-100
1mm	τ_{225}=0.06	2.0	7.9	14	>>
2mm	τ_{225}=0.1	2.8	35	68	>>
4mm	τ_{225}=0.19	5.1	700	1600	>>

On this table, yellow indicates the NEFD is a factor 2 or worse than nominal and red is more than a factor 3 worse.

There are often significant diurnal, seasonal, and longer-term (e.g. El Nino) effects – often a factor of 2 in PWV; some sites are more variable than others. But very roughly, the following sites give a reasonable fraction (up to ~50%) of time where the PWV is equal to (or better than) the value indicated. *At this stage the values are a very rough guide; different authors give different answers, and the variations are large.*

Table 21: Examples of ranges of pwv for various sites

PWV *	"Typical" site	Reference
0.35mm ±0.2	Antarctica (3000m)	http://astro.uchicago.edu/cara/research/site_testing/submm.html
1.2mm ±0.5	Chajnantor (5000m)	http://alma.sc.eso.org/htmls/sumary9899.html
1.8mm ±1	Mauna Kea (4200m)	http://puuoo.caltech.edu/tau_plot.html
~3mm	Paranal (2500m)	http://www.eso.org/paranal/site/paranal-figs.html#water
~4mm	Pico Veleta (3400m)	http://iram.fr/IRAMES/otherDocuments/manuals/manual_v20.ps

- Note: the PWV is the range of the 25 and 50% quartiles, averaged over Winter and Summer.

8.3.1 Is 0.5mm PWV unreasonable to expect?

The baseline assumption for the science case and sensitivity estimates is 0.5mm pwv. Is this unreasonable to expect from an ELT site? The plot shown below shows the pwv measured over the past week, from the APEX telescope on Chajnantor (the ALMA site). This was taken from the APEX web page (http://www.apex-telescope.org/weather/index.html) on June 2006 when this report was being written. Clearly pwv<0.5mm can be seen from this site over sustained periods.

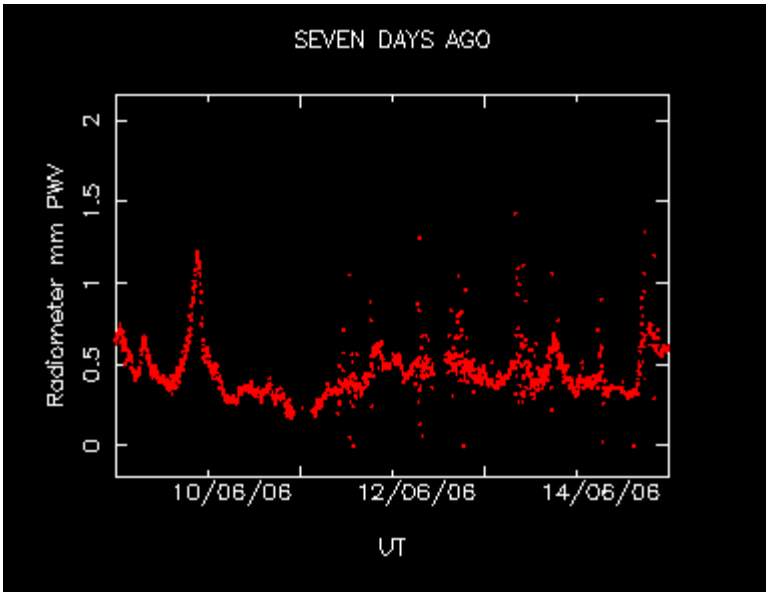

Figure 21: Plot of pwv over a period of a week from the APEX site.

8.3.2 Is 200µm a viable window?

Based on the above estimates, the 230 or 200µm windows may be usable for pwv~0.5mm. The range of 200µm sensitivities in Table 20 reflects the uncertainty in the model and observations. Also the assumed atmospheric transmission is at the band centre, so a mean value over the band will depend on the filter bandwidth. However, with atmospheric transmission of only ~10% (see Figure 19), it is likely that the calibration in these conditions will be very uncertain, making such observations of limited use. These windows become useful for astronomy for pwv<0.3mm. Such conditions do occur on sites such as Chajnantor (see above), but more extensive site testing would be needed before deciding whether the number of useful days with these conditions warrants inclusion of this band in SCELT.

8.4 Tradeoff between ELT site and telescope diameter

The telescope site is by far the most critical aspect of the observatory for the submillimetre. This is illustrated in the following tables which show the sensitivities of SCELT as a function of pwv and telescope aperture for 450 and 850μm.

The important point from this table is that at 450μm, a 30m ELT on a good site (0.5mm pwv) is as sensitive as a 42m ELT on a mediocre site (1mm pwv), and more sensitive than a 60m ELT on a poor site (2mm pwv).

Indeed, the sensitivity of a 30m ELT on a good site would be similar to that of a 100m telescope on a poor site. This does not apply at 850μm, where the site is less critical.

	D = 60m	**42m**	**30m**
PWV = 0.2mm	1.2	2.4	4.7
0.5mm	1.8	3.8	**7.3**
1mm	3.9	**7.9**	15
2mm	**17**	35	69

Table 22: 450μm sensitivity as a function of telescope diameter and pwv. Note the similarity in sensitivity of 30m/0,5mm and 42m/1mm.

	D = 60m	**42m**	**30m**
PWV = 0.2mm	0.8	1.6	3.1
0.5mm	0.9	1.8	3.5
1mm	1.0	2.0	3.9
2mm	1.4	2.8	5.5

Table 23: 850μm sensitivity as a function of telescope diameter and pwv.

8.5 Seeing and AO requirements

The variations in the position and "Strehl ratio" of a telescope beam at submm wavelengths are dominated by variations in the PWV content over different parts of the aperture. This is most evident with submm interferometers such as the SMA (and eventually ALMA), where corrections for varying water vapour content will be made for each element independently, and used to make corrections in the final cross correlation. A study of the effects on the SMA has been made and is described in http://sma-www.cfa.harvard.edu/memos/tech_no.html Memo 154. Table 18 compares the submm seeing (under median conditions for the SMA) with the SCELT resolution. The so-called "anomalous seeing" effects occur when the atmosphere is more unstable, generally at Sunrise and Sunset; they can be several arcsec, even on good sites.

The timescales for the submm seeing variations are set by the time for water-vapour clumps to cross the aperture (in the near field). For winds of 20km/hr (5m/s) this would be ~20 seconds.

The results indicate that to first order, except for possibly the very shortest wavelengths, average sub-millimetre conditions would not affect the beam. To maximise the possible range of observing conditions, the possibility of a sub-mm seeing correction should be investigated.

Table 24: Submm seeing (based on SMA Memo 154)

Wavelength	Submm seeing (median conditions on Mauna Kea)	Submm seeing (poor conditions, Sunrise/Sunset)	SCELT diffraction limited beam
850µm	0.9"	~10"	5.0
450µm	1.1"	~10"	2.6
350µm	1.2"	~10"	2.1
200µm	(1.4")	~10"	1.2

8.5.1 Submm seeing measurement and correction

The water vapour variations do not affect the optical refraction (to 1st order), so submm seeing measurements cannot be made with optical guide stars. However SCELT could employ the same technique as used by interferometers, by measuring the atmospheric emission at different points over the aperture, and correcting the telescope tip/tilt or low-order AO corrections. This is the "Water-vapour-AO" system mentioned in RD05.

Tip/tilt corrections

Corrections would have to be made on a 20-second timescale. This could be done by moving the telescope (tip/tilt), or feeding the information to the DR system, for corrections in the regridding algorithm. The latter software correction would be

acceptable. Four water-vapour monitors could be used at the edges of the aperture – or two differential ones for each axis.

AO corrections

This could only be done using the primary or secondary actuators, in a low-speed (0.1-1Hz) high-amplitude (1-10 arcsec) mode. It would require multiple water-vapour monitors over the aperture.

Submm guide stars

The submm number count suggests that over a 5 arcmin fov, there will be ~20 background galaxies at or above 10mJy. These may be point sources, or contain a significant compact component, but the sensitivity is such that the s:n will be ~10σ on these in ~1 second. Thus they could be used as "guide stars" for shift-and-add, to remove both flexure and submm seeing. This is dependent on the exact background number count model and their size distribution, but these confusing sources may be put to good use. Cross-correlation of the whole-field structure in individual frames might be the most sensitive way of doing this measurement, as it takes advantage of all the lower-level background structure. This would need to be investigated further.

8.6 Additional telescope requirements

8.6.1 Telescope velocity and acceleration

An additional telescope requirement for SCELT operation in the scan mapping mode is that the telescope sky coordinates should be available in real time, at a 200Hz rate. This is to allow the telescope to be scanned over the sky, in some defined but potentially complex motion, whilst taking data continuously and regridding into the final image. See section 12.3.

The data rate for efficient sky removal is 200 frames/second. The required telescope velocity and acceleration are given in the following table.

Table 25: requirements on telescope velocity and acceleration

	Requirement	**Goal**	**Notes**
Telescope scan velocity	50 arcsec/second		For scan mapping
Telescope acceleration	100 arcsec/second^2		For high efficiency, scan using Lissajous figures

Note that the observing modes planned for SCELT (and SCUBA-2) do not require any chopping or nodding of the telescope.

8.6.2 Daytime observing

Unlike optical and the near infrared, submm observing can frequently take place efficiently during the day. The main astronomical limitation is the atmospheric stability. On Mauna Kea, the sky is stable enough to allow daytime observing time to continue to 9

or 10am local time, and on exceptional days, observing can continue all day. Thus ELT would be utilised more efficiently, potentially resulting in 10-30% more observing time and scientific output from the observatory. However, this operation places two significant requirements on the telescope and observatory:

- The alignment of the individual telescope segments must be maintained to the desired accuracy (to maintain <2 arcsec beam size) without the use of guide stars. Using the standard Ruze formula requires accuracy of λ/20, or 10μm rms. Possibly this could use a lookup table although the effects of wind would need to be considered.
- Careful sun avoidance systems would obviously be required. This would not only be for the primary and secondary, but also all the concave mirrors. The effect of solar heating on the telescope structure would need to be investigated.
- Fast and efficient switchover to daytime/sub-mm observing is needed.

8.7 Instrument data rate

From the SCUBA-2 studies, a frame rate of 200Hz is required for the TES detector readout. Some data compression is possible, to reach ~3 byte words. For example, for 2 arrays of 50k and 85k pixels (for 450 and 350μm), the total data rate from SCELT will be 140,000 x 200 x 3bytes, = 80Mbytes/second, or ~3Tbyte/night. This is a sustained rate, as most observing requires scanning and fast readout.

9 Instrument concept design

9.1 SCUBA-2 as a SCELT prototype

The baseline design of SCELT presented here is based on the SCUBA-2 concept. So in some respects SCUBA-2 can be regarded as a "prototype" for SCELT; this has the advantage that several of the high-risk areas will be tested once SCUBA-2 has been commissioned and is running reliably on the JCMT (likely to be ~2007-2008). Areas where we would expect particularly useful feedback for the SCELT project are the calibration method, observing techniques, cooling system, and overall design.

However, we are projecting advances in detector technology and assume that focal plane bolometer arrays will exist for SCELT which will have ~100,000 densely-packed pixels. This also requires that such an array can be cooled with reasonable technology. This is the main area where SCELT will be significantly different (and where it differs from the OWL baseline concept).

Note also that the optics design as outlined here is based on a 30m primary. Changing to a 42m primary (as assumed in most of the science case above) will have the following effects on the design:

- Proportionally larger optics
- Larger filters, windows
- Larger cryostat
- Larger heat loads

None of these is thought to be a show-stopper. Further detailed work would be required to revise this optics/mechanical design for the larger 42m concept.

9.2 Optics

9.2.1 Optical concept

The optical concept of ELT is based on a all-reflective optical design using the F/6, 30-m telescope ELT as the input to the instrument. There is 1 warm mirror N1 producing a beam entering the cryostat through a window and a cold stop at 4K. The cold mirror N2 relays the F/6 telescope focus to the F/4 beam on the detector.

Specification:

- Telescope: ELT diameter: 30-m
  F/16
- SCELT: wavelength range: 350- 450μm primary.
- FOV: 5x5 arcmin
- Pixel size ~λ (ie 0.2mm for 200μm, 0.5mm for 450μm)

- Pixel spacing: 0.6 λ/D (Nyquist sampling)
- Plate scale: set by the wavelength

For this report, we have designed SCELT as a dual-band 450/350μm instrument, these being the primary bands. Inclusion of a 3rd band at 850μm (or possibly 200μm) could be done either with a filterwheel, or with a second dichroic.

9.2.1.1 Optical layout

This is shown in the following two diagrams.

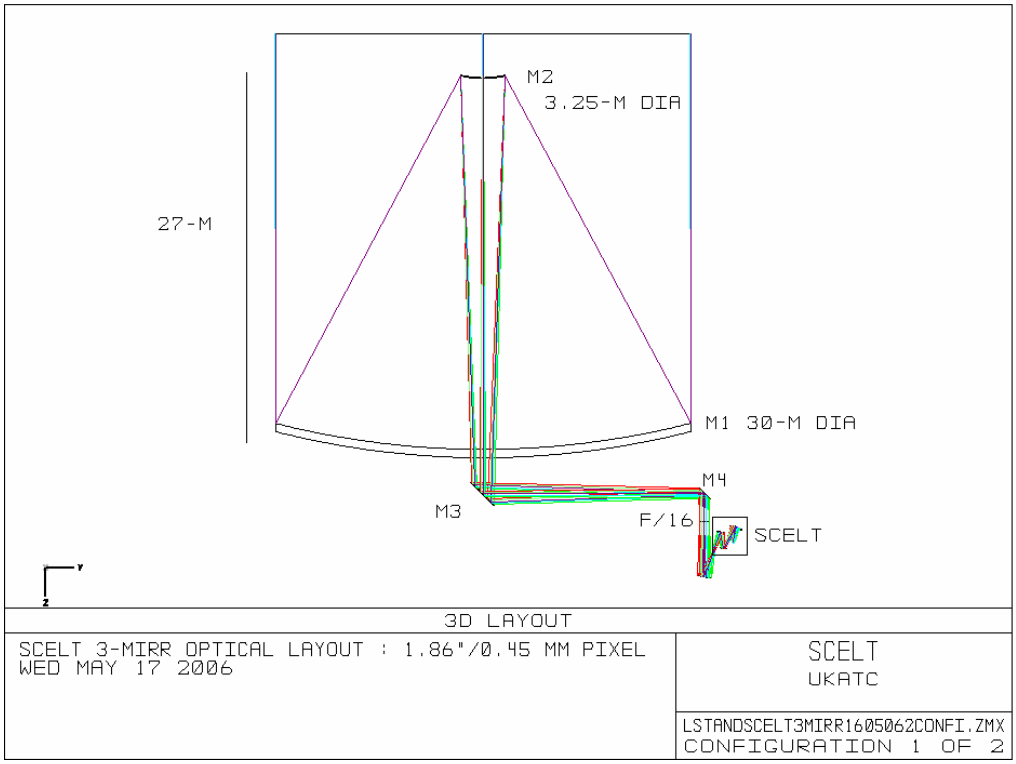

Figure 22: ELT with SCELT at Nasmyth focus

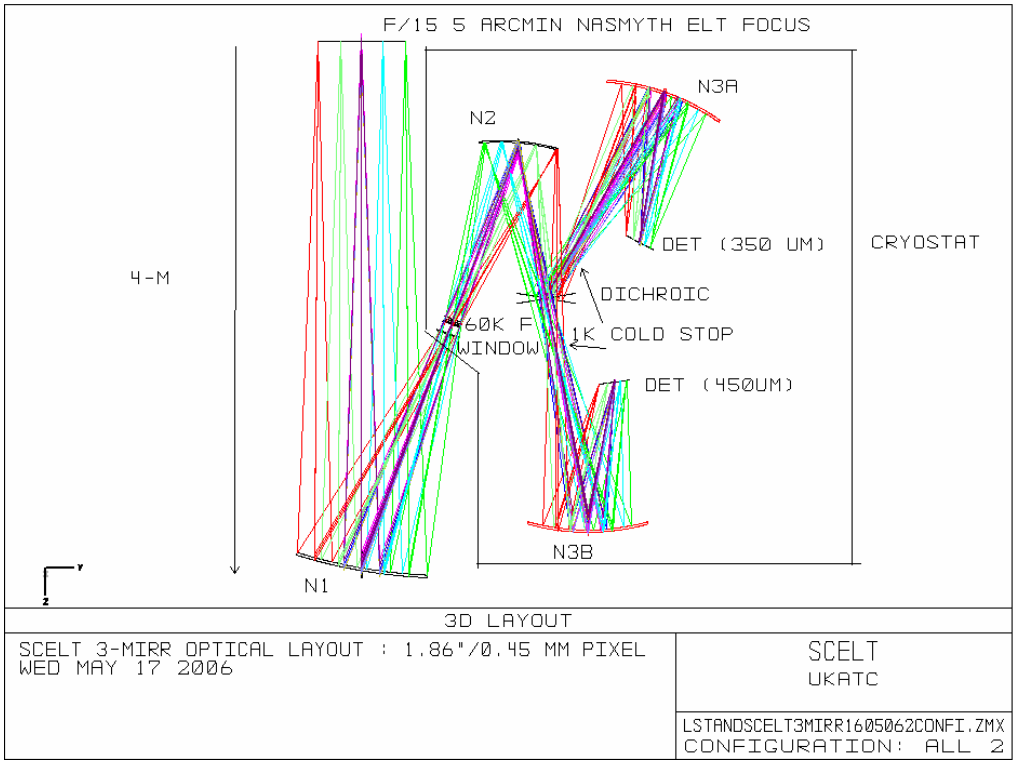

Figure 23: SELT optics layout with 2 dichroics

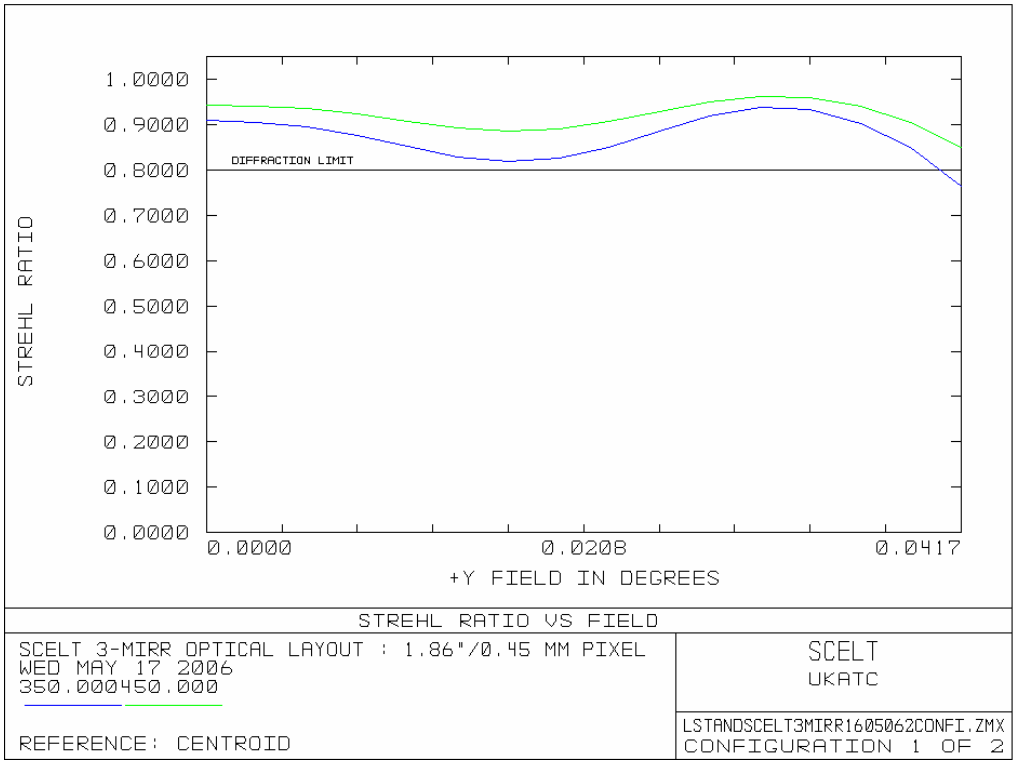

Figure 24: Strehl ratio for 350 and 450µm

9.2.1.2 Optical data:

The biconic Al mirrors are manufacturable with the present technology used on SCUBA-2 mirrors, the window and the filters are under study concerning their manufacturability. The current max size for the filters is around 200-mm.

9.2.2 Spot diagrams

The Airy disk (defined by 2.44 λF) is shown around the spot diagrams. Spots are inside the Airy disks which means that the optical design will give diffraction limited images. Coma and astigmatism are the dominant geometrical aberrations and could be compensated by the active telescope to improve the image quality.

9.2.3 Conclusion

The SCELT preliminary optical concept meets the image quality requirement (diffraction ltd system for the working wavelength) for the 5 arcmin FoV. The manufacturability of the window and filters still remains an issue. A number of options which may optimise the design even further include investigating the use of:

- Position of waveplates for polarimetry
- Position and number of filters

10 Mechanical

TBD

10.1 Thermal

The baseline option uses large KIDs arrays (see section 11.1). These will use frequency-multiplexed readout systems at ~4-8GHz. So the readout is through semi-rigid coax assemblies. Current projections suggest ~100 such wires from the detector to room temperature for the ~100,000 pixels of SCELT.

11 Electronics

11.1 Detectors

The choice of detectors is important. It affects the maximum field of view achievable, the pixel density on the sky, the cooling requirements, and the optics design.

The requirement is to Nyquist-sample the sky, ie 0.6λ/D spacing. This gives the following array sizes for a 42m primary and 5x5 arcmin fov. The array size will scale as the telescope aperture^{-1} for the same fov.

Table 26: SCELT detector requirements

Wavelength	Detector spacing (arcsec)	Detector size (pixels on a side)	Approximate number of pixels
200 μm	0.6	500 x 500	250,000
350 μm	1.1	290 x 290	85,000
450 μm	1.4	225 x 225	50,000
850 μm	2.5	120 x 120	15,000

There are three options for submm detectors for SCELT:

1. Use existing detectors. This largest chips are currently the TES arrays on SCUBA-2, which are 40x32 detectors, 4-way buttable, giving a total of 5120 pixels per focal plane array. This might then be expandable by a factor of 4 by butting together the FPA assemblies (see the SCOWL design study). However, this would yield a low filling factor for the field of view (around 30%) – essentially very large gaps in the array.

2. Use a gradual development of existing detectors. Possibly the TES architecture could be expanded by a factor of 2 in each dimension, by using larger wafer sizes and better yields building on experience with SCUBA-2. This might give 80x64 per chip, or ~20,000 pixels per focal plane array. This meets the pixel count for 850μm, but not for the short wavelengths. It has the advantage over (1) of having a high filling factor of the focal plane (~80-90%). But requires technology development, and will not meet the pixel count requirements at 450μm.
3. Develop other technologies, such as KIDs. The potential for larger-format arrays will be greater, and we might predict a truly large-format FPA with pixel counts in the 100,000 region. This is new technology, and so represents a considerable risk. However, other groups such as Caltech and NIST are also looking to such larger-format KID arrays, so we might expect considerable development over the next few years, in time for SCELT.

The following sections will describe the TES and KID options in more detail.

11.1.1 Transition Edge Sensor detectors

Recent advances in detector technology have demonstrated that large-format arrays of many thousands of pixels are now possible so that wide-field submillimetre imagers are more feasible. Indeed there are a few projects, currently underway, utilising the advances in this field. One of these instruments is SCUBA-2, a new generation camera under development for the JCMT. A substantial detector development programme, for SCUBA-2, is currently underway at the National Institute of Standards and Technology (NIST) and the Scottish Microelectronics Centre (SMC). The detectors are state-of-art transition edge sensors (TES) hybridised to a Superconducting Quantum Interference Device (SQUID) time-division multiplexer, shown in Figure 25.

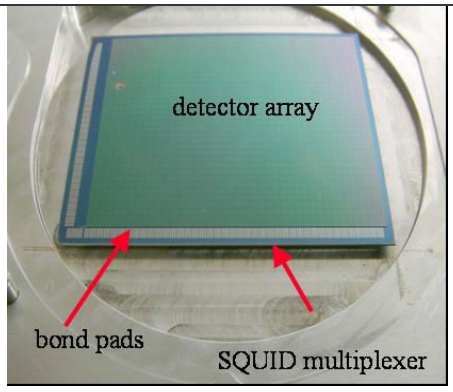

Figure 25: Hybridised detector/multiplexer

The TES is a superconducting thin film biased in the transition between the normal and the superconducting states. If biased in the transition region a small change in temperature will lead to a large change in resistance as shown in Figure 26. The detector is held at a constant voltage bias so that a change in resistance will cause a change in current which will be coupled into the SQUID readout.

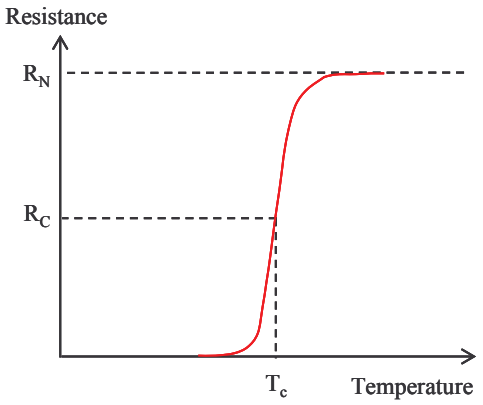

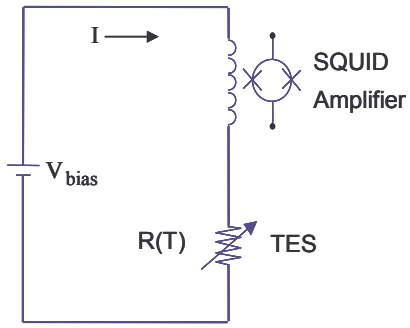

Figure 26: (a) R-T curve for TES device (b) TES bias circuit

The TES devices are low impedance and therefore less susceptible to microphonics and operate faster than conventional bolometers due to their high sensitivity and electro-thermal feedback mode of operation. The advantage of the SQUID multiplexer is that they consume less power than conventional FETs and operate at the same temperature as the detector. This last point is very important for arrays of detectors as it allows the readout of the pixels to be undertaken with a practical number of wires.

Without the advantage of multiplexing, each pixel would require 6 wires which would lead to >100,000 wires being routed from all of the detectors required for SCUBA-2, which would cause considerable problems in instrument building. Even with multiplexing a total of ~2500 wires are still needed to route signals to/from the detector arrays within the SCUBA-2 cryostat. For each detector subassembly (40x32 pixels) there are a minimum of 320 connections required and SCUBA-2 has two focal plane units of four detectors each. A focal plane unit with the four detector subassemblies is illustrated in Figure 27.

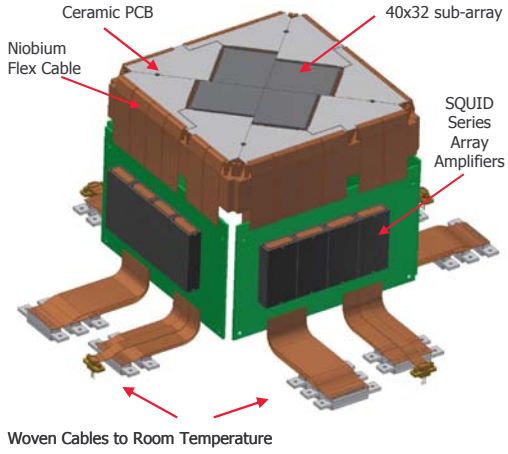

Figure 27: SCUBA-2 Focal plane unit

The specification of the current SCUBA-2 detector devices are as follows:

- Pixel size 1.135mm^2
- Physical size ~ 40mm x 50mm
- 1312 pixels per detector (40 rows x 32 columns + 1 'dark' row)
- 2 sides buttable – allows a mosaic of 4 detectors (5120 pixels)
- Operating wavelength: one mosaic at 450um and one mosaic at 850um
- NEP $_{(450um)} < 15x10^{-17}$ W/√Hz, NEP$_{(850um)} < 3.5 x10^{-17}$ W/√Hz
- Operating temperature 100mK

Wavelength range - Continuum detectors of this type are efficient at wavelengths between 200um to 1mm. The wavelength of operation is dependant on the geometry of the pixel, in particular the thickness will determine the operating wavelength. This in turn affects the absorption efficiency (which is equivalent to QE). The interdependencies of all the parameters and geometries is quite complex but detectors for operating at 350um, 450um and 850um are realisable.

The design for SCELT would be to forgo the costly and time consuming development work and use the existing SCUBA-2 design. Even with this approach dealing with the heat load, in the focal plane, from the increase in number of pixels and the increase in read-out wire count will be a challenge.

Figure 28 shows a schematic layout of four SCUBA-2 type detector subassemblies which would be required to cover the SCELT field-of-view. This would give a total of 20480 pixels.

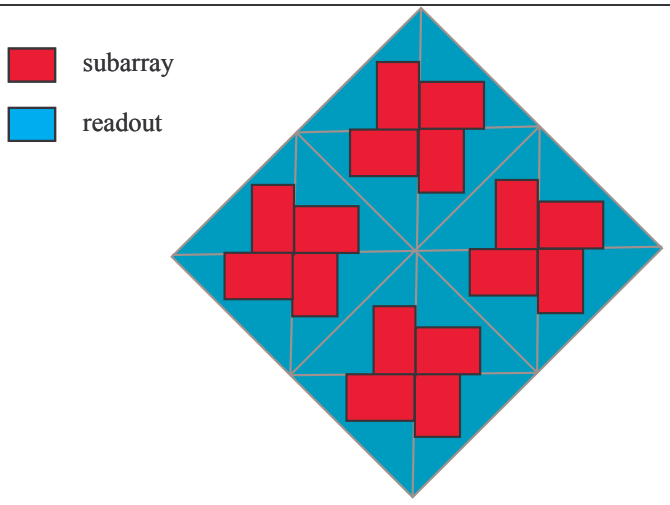

Figure 28: SCELT Focal Plane schematic layout

With the present development programme, focal plane units consisting of 20k pixels are realisable. To significantly increase the number of pixels would require a substantial development programme and may be achieved in a timescale which will be of benefit to SCELT.

11.1.1.1 Readout Electronics

As shown in Figure 27 each detector is wire bonded to a ceramic PCB which is connected to a further PCB housing part of the readout electronics, the SQUID series arrays. This connection is made via niobium flexible circuits, which goes superconducting at temperatures below 9K. Cryogenic ribbon cables, constructed from niobium wires weaved with nomex fibres, route the signals to room temperature electronics. The detector output is DC-coupled to the readout electronics.

Mounted on the outside of the cryostat would be a VME rack containing all the circuitry to control and readout the detector. Fibre optic cables connect the warm readout electronics to a control and image capture PC running Realtime Linux.

Each VME rack contains a Clock Card, Address Card, 3x Bias Cards, 4 x Readout Cards, Power supply card and one VME rack will readout 1 detector therefore sixteen racks of electronics would be required for SCELT for each waveband.

11.1.1.2 Development of TES detectors for SCELT

In terms of the current SCUBA-2 array design there are four main issues to be overcome to realise even larger format arrays: (1) processing of silicon wafers (2) device density on the multiplexer wafer (3) power dissipation in focal plane (4) the large volume of readout wires.

Processing capabilities are limited to 3" wafers due to fabrication limitations within the project. This limits the number of rows of detectors to 40. Also, at present the size of wafers that can be successfully hybridised is about $50mm^2$. Increasing the number of rows would also affect the multiplexing frequency which in turn affects the SQUID coil design. The detector is two edge butt-able, limiting the configuration to a mosaic of four.

Also for efficient coupling to the antenna, the detector pad assembly cannot be significantly smaller than the wavelength itself. So for 50x50mm wafers, this means 55x55 pixels at 850μm, and 100x100 at 450μm. However there is a further limitation to the minimum detector size, set by the size of the SQUID readouts to ~1mm each pixel. Further development would be required to increase the pixel density, in order to realise the 100x100 array for 450μm on a 50mm wafer.

The net effect of these factors is that to increase the size of this type of detector would involve further development work, likely using 6" wafer technology.

11.1.1.3 Wire count and heat load from TES arrays

The SCUBA-2 arrays (total 10,000 detectors) require 2500 wires, which is near the limit of heat load and complexity. Dumb scaling of these arrays to 100,000 pixels would therefore imply 25,000 wires. Higher levels of multiplexing would be necessary to realise readout from such large TES arrays.

11.1.2 KIDs arrays

An alternative to the SCUBA-2 TES detectors for the detection of submillimetre radiation would be Kinetic Inductor Detectors (KIDs). They comprise a superconducting thin-film

transmission line resonator. When a superconductor is operated well below its transition temperature (T << Tc) incoming photons are absorbed, breaking cooper pairs and creating a large number of quasi-particles. This increase in quasi-particles density changes the surface impedance, which is mainly inductive. This change in the surface impedance is measured by incorporating the superconductor into a LC resonant circuit. The change in surface impedance alters the resonance frequency and can be monitored by the RF readout system. By loosely coupling a large number of resonators operating at slightly different frequencies, to a single thin-film transmission line a large number of pixels (>1000) can be read out through a single HEMT amplifier and coax line. The number of frequencies that can be multiplexed depends on several factors (1) bandwidth of HEMT amplifier (2) typical Q of resonator (3) lithographic processes (4) exciting frequencies, to name a few. The advances made in wireless communication means that the RF readout and data acquisition could be implemented with mainly of-the-shelf components.

A number of international groups are working on developing KIDs. In the US groups at JPL and Caltech are working in this area as well as a group in the Cavendish Lab at University of Cambridge. Most of this work has concentrated on the X-ray region mainly because the high photon energies allow single-absorption events to be recorded rather than there being any reason that KIDs are more suited to working at this wavelength. Indeed KIDs can be configured to work at submillimetre, infrared, optical and X-ray wavelengths (RD07-10).

This technology is still in the early development phase but within the next 3 years it is likely that a 32 element system suitable for use in the submillimetre will be demonstrated, along with a suitable readout system that will scale to the larger format arrays.

The advantages of KIDs over TES detectors is that they are easier to manufacture and likely to be cheaper as the TES has the costly and complex hybridisation of the detector to the SQUID multiplexer. KIDs also have a future potential to be extended to large format arrays subject to ongoing development programmes.

Another advantage is that frequency multiplexing can be used to readout many detectors using a single HEMT amplifier thereby significantly reducing the heat load from the number of interconnections required as well as the practical problem of routing the connections through the cryostat (see below).

The advantage of TESs over KIDs is that they already have been shown to be effective in the submillimetre regime and are sufficiently far along in development. But on the order of 3 years the KIDs development may be sufficiently mature to be seriously considered as an alternative to the TES detectors for SCELT.

11.1.2.1 Coupling of KIDs to beam

Two options:

1. antenna coupling, in which case the pixel separation may be larger than 0.6λ/D (possibly as much as 2λ/D) to get good efficiency. This has the disadvantage that the fov is sparsely sampled, lowering the overall sensitivity of the camera and requiring dithering or jiggling to fully-sample the image.
2. coupling using an absorption pad, similar to the TES detectors. This has the advantage of being able to closely pack the detectors, but has not been investigated in detail for KID arrays.

11.1.2.2 Wire count and heat load from KID arrays

KIDs use frequency-multiplexing readout at GHz frequencies. This would require semi-rigid coax or balanced pair RF readout cables. The number of pixels which can be frequency-multiplexed on a single coax is set by the Q of the KID resonance and the photolithography tolerances. For $Q \sim 10^5$ (a few 10^4 is currently possible, so 10^5 is probably achievable in the next few years), a readout centre frequency ν=5GHz, and specifying a channel frequency separation of 10x the resonance width to avoid cross-talk, then the channel separation would be $\Delta\nu \sim 0.5$MHz. Photolithographic techniques for KIDs manufacture are likely to limit the channel separation to >0.25MHz. So for a readout bandwidth, bw, of 2GHz, the number of possible channels would be $bw/\Delta\nu = 4000$. The total number of pixels in SCELT will be ~100,000 and so require ~25 RF cables from the detectors out to room temperature. This will set a considerable heat load, and will need careful staging of the link from 100mK out to ambient. For example, with HARP (a 16-beam heterodyne array with RF cables at 4GHz) the heat load from the wires from the 20K to the 4K stages was ~30mW.

Summary of KIDs advantages:

- Easier to manufacture
- Wire count down, so simpler & more robust wiring design
- Fewer wires, so potentially lower heat load (but requires RF cables with low heat conductivity, so this would need further investigation)
- Potential to fully populate the field of view, increasing the number of pixels by ~5
- Potentially cheaper to procure
- May have lower detector NEP compared with TES detectors

12 Observing modes

A brief outline of the main data-taking modes is as follows.

Record flat-field illumination – a source of radiation is inserted in the beam to provide uniform illumination to the arrays and to provide the basis for calibrating the bolometers relative to one another.

Calibration with dark shutter closed – the cold dark shutter is closed isolating the bolometers from all radiative power input. Measurements are then taken at various setting of the pixel heaters to determine the response curves of the bolometers.

Atmospheric extinction calibration – measurements are taken of the flux from the sky at a range of zenith angles in order to separate the Earth's atmospheric emission from telescope emission. This allows the Earth's atmospheric emission to be determined directly from science frames, and the atmospheric extinction can then be calculated.

Mosaic map – a series of CCD-style exposures of the science field are taken interspersed with adjustments to the telescope position to make a mosaic which fills-in the gaps between the subarrays.

Scan map – data frames are recorded continuously at 200 frames/sec while scanning the telescope over the science area.

Telescope pointing – check and adjust telescope pointing by imaging a bright point source on one of the subarrays.

Telescope focus – check and adjust telescope focussing by imaging a bright point source on one of the subarrays.

Mosaic map polarimetry – a polarimeter version of mosaic map. The half-wave plate is spun at about two revolutions per second, resulting in the polarised signal being modulated at 8Hz.

Scan map polarimetry – a polarimeter version of scan map.

The various observing modes suggested for SCELT are being developed for SCUBA-2 and will be tested when that instrument is delivered.

12.1 Field Rotation

SCELT will not require a field rotator. This is handled by taking images rapidly and correcting for field orientation in software, which is the approach used at JCMT and most sub-millimetre telescopes. The detectors are non-integrating devices and so acquiring data with a high frame rate is unavoidable even in the absence of field rotation.

The addition of a turntable suitable for SCELT would have some advantages (mosaic and scan patterns would not need to rotate relative to the astronomical image) but this is not a major issue.

12.2 Mosaic Maps

If full sampling of the field-of-view is not possible due to slow developments in detector technology (see section 11.1), the physical construction and mounting of subarrays will likely leave large gaps in the coverage of the focal plane. The most straightforward way to overcome this is to fill-in the gaps by taking a series of data frames at various telescope offsets. The data frames have to be corrected for pixel-to-pixel electrical zero point drifts by reference to a recent dark measurement. This requires the zero point drifts to be smaller than the photon noise averaged over the interval between dark frames. The feasibility of this mode clearly depends upon the array stability, which is a factor yet to be determined as part of the SCUBA-2 project for TES detectors.

12.3 Scan Maps

The scan map technique, whereby data frames are acquired rapidly while the telescope scans over the science area, is useful both as an alternative way of filling the gaps between subarrays and as a method for making maps of areas larger than the focal plane. The technique is heavily dependent upon having a suitable map reconstruction algorithm. The

method results in any sky pixel being measured by multiple bolometers, and this can be used to determine the relative bolometer zero points independently of taking dark frames.

A key factor is the pattern of scanning used, and the ability to tag each of the 200 frames recorded per second with the corresponding telescope position. Astronomers using the SHARC-II instrument have studied various scanning patterns, and have concluded that, for smallish maps, Lissajous figures have good properties with respect to avoiding excess telescope accelerations (in general telescope position uncertainties become unacceptable at high accelerations).

Alternative scanning strategies and matching image reconstruction techniques are being studied for SCUBA-2, making careful use of the advances made by the SHARC-II team.

12.4 Polarimetry

It is expected that successful polarimetry will require spinning the half-wave plate at a sufficient speed that 1/f noise due to the Earth's atmosphere is significantly below photon noise. In the sub-mm, measurements at 8Hz are expected to be sufficient, which means spinning the half-wave plate at two revolutions per second. A dominating feature of the raw data will be the polarising effect of the telescope optics on the sky background, which will produce a linearly polarised signal many orders of magnitude brighter than the required science signal. Handling this requires accurate relative calibration of the bolometers.

For SCUBA-2, people are also considering the possibility of a scan map mode for making polarisation maps of extended sources. The feasibility of this is speculative at present.

13 Software

The software system block diagram assumes the telescope will adopt the usual

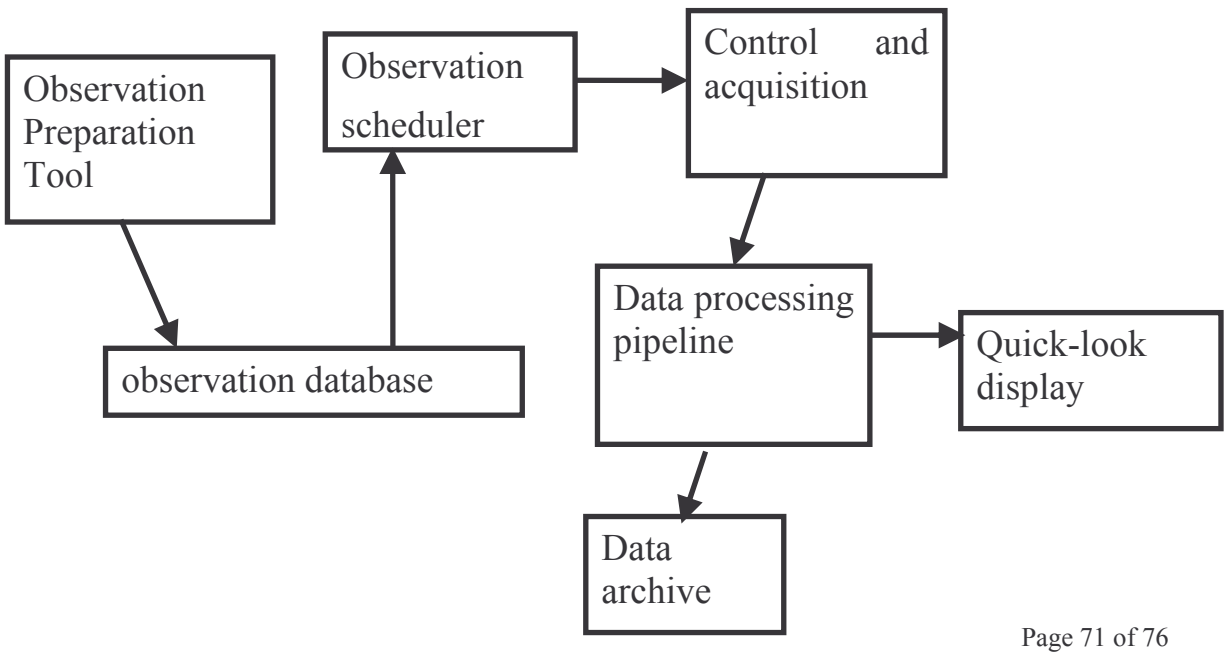

architecture, whereby observation requests are prepared ahead of time and stored for subsequent recall at the telescope, and the data acquired are processed automatically by a data processing pipeline. As always, this carries the requirement that the data written by the control and acquisition subsystem contains all the information needed to drive the pipeline, including the identification of processing recipes if necessary.

13.1 Calibration

If TES devices are used, the exact calibration technique will depend on experience with SCUBA-2 on JCMT, from 2006 onwards. If other devices such as KIDS are adopted, the calibration technique is likely to be similar, although further modelling would be required.

13.1.1 Relative Calibration of Bolometers

The bolometers are nonlinear devices and their response curves are expected to differ slightly from bolometer to bolometer. In addition, drifts in electrical zero points can be expected.

Flatfielding will be required, using a calibration wheel or chopper assembly.

13.1.2 Extinction Correction

In the submm, atmospheric emission and extinction are both dominated by the opacity of water vapour. Therefore, there is expected to be a tight correlation between the flux recorded from the atmosphere and the extinction, and this is confirmed by detailed modelling. Provided an absolute calibration of the power received can be achieved, it becomes possible to calculate the atmospheric extinction directly from the sky background recorded in the science data frames. The calibration involves knowing the non-atmospheric flux present in science frames – this is normally grouped under the heading “telescope emission”.

This technique is not yet standard and has to be proved using SCUBA-2. If it proves nonviable, then the system will require a water vapour radiometer to provide a measurement of the atmospheric extinction.

14 Management

The management aspects of this report are focussed on providing a first basic estimate of the cost for producing SCELT. As such the estimate must be treated with great caution due to the very early stages of the concept. As SCELT will be a brand new instrument, data on costs have been inferred by drawing comparisons with SCUBA 2 which is now in the AIV phase. Assumptions are provided to help establish the background to making the estimates.

14.1 Assumptions

The following assumptions have been made:

1. No allowance for inflation has been included; therefore all cost estimates are at 2006 prices.

2. A consortium based on the original SCUBA 2 team (or people with equivalent skill sets) is used to produce the detectors.

In global terms:

1. Overall design effort is expected to be of a similar order as for SCUBA 2 with potential to reduce because of what has been learnt on SCUBA 2.
2. AIV in Europe is expected to be generally comparable to the effort for Scuba but will need to be scaled for the increase in effort required to integrate more detectors.
3. Activities at the Telescope site that could have a bearing on acceptance timescales of the Instrument have not been included (i.e. we assume for estimating purposes to avoid double accounting with the Telescope commissioning activities that all the infrastructure such as services and software is available).

14.2 Costs

The effort required to produce SCELT has been provisionally estimated using the experience from the SCUBA 2 programme. It should be noted that there are three main sites involved with developing SCUBA 2 in the UK and one in Canada. In addition, essential input has been provided by other partners in the USA with regard to the detector technology. An exchange rate of €1.5 to the £ has been used.

- At present it is envisaged that effort would cost of the order of €10,000k.
- At present it is envisaged that hardware would cost approx €20,000k (of which €10,000k is for the detectors and development).

For SCELT there are currently significant issues which have been identified for some of the hardware items which could necessitate an increase to these costs should dedicated R&D programmes funded by the project be required to solve manufacturing issues.

14.2.1 Contingency

An overall allowance for dealing with unknown risk must be included within the estimates. Current experience indicates that this should be of the order of an additional 20% for effort and 10% for hardware for a mature concept.

15 Conclusions

TBD

16 Appendices

Annex 1: Technology Development Areas

The following table lists the issues that have been identified so far during the study on SCELT. Cross-references to sections in the text where the issues are discussed are provided.

#	Issue	Comment	Section Cross-Reference
1	Size of input window that can be manufactured	Needs Technology Development Programme	
2	Size of filters and dichroics that can be manufactured	Current size of SCUBA 2 filters are approx 200mm; 300mm is possible but 400mm is needed for SCELT Needs Technology Development Programme	
3	Polarimetry wave plates	Need waveplate of ~800mm diameter, no means of manufacturing this just now Needs Technology Development Programme	
4	Waveplate rotation	Fast (2Hz) rotation of a large waveplate would be needed.	
5	Detector Coolers	Dilution refrigerator used for SCUBA-2. This may be enough, but more estimates of thermal loads from detectors required.	
6	KIDS or alternative detectors	Development of alternative detectors has the potential to reduce cost and complexity of cooling. An improvement in performance is also likely due to increased packing density .	

Annex 2: Telescope requirements generated by SCELT

The following system level requirements have been identified as being necessary to allow SCELT to gather the science based on the presented concept. This should help contribute to the system level trade-offs debate.

#	SCELT System Need	Resulting System Requirement	Comment
1	Site quality (pwv)	≤0.5mm pwv	Highest priority, for 450 & 350μm operation
		≤2mm pwv	For 850μm operation
		≤0.3mm pwv	For 200μm operation
2	Telescope diameter	42m primary is 2x more sensitive and has 2x lower confusion compared with 30m.	Site is more important than diameter as far as sensitivity is concerned.
3	SCELT has the potential to be used during daylight	Means of telescope tracking and maintenance of a surface accuracy of λ/20 (=10μm) during daylight required	
4	Potential hitchhiker mode	Sub-mm/optical-ir dichroic	
5	Scanning velocity and acceleration	Velocity: 50arcsec/sec (max) 15arcsec/sec (typical) Acceleration: 100arcsec/sec/sec	For scan mapping. The maximum scan rate gives critical sampling by a single bolometer, but oversampling and a slower scan rate is preferred. The key thing is that the telescope instantaneous position must be well-determined.
6	Submm seeing	<1 arcsec May need method of sub-mm "tip-tilt" correction	See section 8.5
7	Instrument Rotator	Not required for SCELT	
8	Flexure	Not a risk, as long as SCELT on a Nasmyth mount	

Annex 3: References

Beichman et al., 2004, Advances in Space Research, vol.34, Issue 3, p. 637

Bernstein et al., 2004, ApJ 128, 1364

Blain et al., 1999 ApJ 512, L87

Blain & Longair, 1993, MNRAS 264, 509

Decin et al., 2003, ApJ, 598, 636

Dullemond & Dominik, 2005, A&A, 434, 971

Dunne et al., 2003, Nature, 4242, 285

Edge, 2001, MNRAS, 328, 762

Edmunds, 2005, George Darwin Lecture, A & G, 46, p412

Greve et al., 2004, MNRAS 354, 779

Helou & Beichman 1990, in ESA, From Ground-Based to Space-Borne Sub-mm Astronomy p 117-123

Hughes et al., 2002, MNRAS, 335, 871

Jewitt et al., 2001, Nature, 411, 446

Jeoung et al., 2005, MNRAS 357, 535

Krause et al., 2004, Nature, 432, 596

Lucas et al., 2005, MNRAS, 361, L211

Matthews & Wilson, 2000, ApJ 531, 868

Motte et al., 1998, A&A 336, 150

Pan & Sari 2005, Icarus, 173, 342

Pearson, 2001, MNRAS, 325, 1511

Siebenmorgen et al., 1999, A&A 351, 495

Su et al., 2005, ApJ, 628, 487

Stevens et al., 2005, astro-ph/0411721

Takeuchi & Ishii, 2004, ApJ, 604, 40

Testi et al., 2003, A&A 423, 323

Wyatt et al., 2005 (in prep)